



UNIVERSITÀ POLITECNICA DELLE MARCHE
Repository ISTITUZIONALE

CD31+ Extracellular Vesicles from Patients with Type 2 Diabetes Shuttle a miRNA Signature Associated with Cardiovascular Complications

This is the peer reviewed version of the following article:

Original

CD31+ Extracellular Vesicles from Patients with Type 2 Diabetes Shuttle a miRNA Signature Associated with Cardiovascular Complications / Prattichizzo, Francesco; De Nigris, Valeria; Sabbatinelli, Jacopo; Giuliani, Angelica; Castaño, Carlos; Párrizas, Marcelina; Crespo, Isabel; Grimaldi, Annalisa; Baranzini, Nicolò; Spiga, Rosangela; Mancuso, Elettra; Ripponi, Maria Rita; Procopio, Antonio Domenico; Novials, Anna; Bonfigli, Anna Rita; Garavelli, Silvia; La Sala, Lucia; Matarese, Giuseppe; de Candia, Paola; Olivieri, Fabiola; Ceriello, Antonio. - In: DIABETES. - ISSN 0012-1797. - 70:1(2020), pp. 240-254. [10.2337/db20-0199]

This version is available at: 11566/284723 since: 2024-12-19T10:31:51Z

Publisher:

Published

DOI:10.2337/db20-0199

Terms of use:

The terms and conditions for the reuse of this version of the manuscript are specified in the publishing policy. The use of copyrighted works requires the consent of the rights' holder (author or publisher). Works made available under a Creative Commons license or a Publisher's custom-made license can be used according to the terms and conditions contained therein. See editor's website for further information and terms and conditions.

This item was downloaded from IRIS Università Politecnica delle Marche (<https://iris.univpm.it>). When citing, please refer to the published version.

(Article begins on next page)

1 **CD31 Positive-Extracellular Vesicles from Patients with Type 2 Diabetes Shuttle**
 2 **a miRNA Signature Associated with Cardiovascular Complications**

3 Francesco Prattichizzo^{+*1}, Valeria De Nigris⁺², Jacopo Sabbatinelli^{*3}, Angelica Giuliani³, Carlos
 4 Castaño^{2,4}, Marcelina Párrizas^{2,4}, Isabel Crespo⁵, Annalisa Grimaldi⁶, Nicolò Baranzini⁶, Rosangela
 5 Spiga⁷, Elettra Mancuso⁷, Maria Rita Rippo³, Antonio Domenico Procopio^{3,8}, Anna Novials^{2,4}, Anna
 6 Rita Bonfigli⁹, Silvia Garavelli¹⁰, Lucia La Sala¹, Giuseppe Matarese^{10,11}, Paola de Candia¹, Fabiola
 7 Olivieri^{3,8}, Antonio Ceriello¹

8 1- IRCCS MultiMedica, Milan, Italy

9 2- Institut d'Investigacions Biomèdiques August Pi i Sunyer (IDIBAPS), Barcelona, Spain

10 3- Department of Clinical and Molecular Sciences, DISCLIMO, Università Politecnica delle
 11 Marche, Ancona, Italy

12 4- Spanish Biomedical Research Center in Diabetes and Associated Metabolic Disorders
 13 (CIBERDEM), Barcelona, Spain.

14 5- Cytometry and Cell Sorting Facility, CEK, IDIBAPS, Barcelona, Spain

15 6- Department of Biotechnology and Life Sciences, University of Insubria, Varese, Italy

16 7- Department of Medical and Surgical Sciences, University "Magna Graecia" of Catanzaro,
 17 Catanzaro, Italy

18 8- Centre of Clinical Pathology and Innovative Therapy, IRCCS INRCA, Ancona, Italy

19 9- Scientific Direction, IRCCS INRCA, National Institute, Ancona, Italy

20 10- Istituto per l'Endocrinologia e l'Oncologia Sperimentale "G. Salvatore", Consiglio
 21 Nazionale delle Ricerche, Naples, Italy.

22 11- Department of Molecular Medicine and Medical Biotechnology, University of Naples
 23 'Federico II', via Pansini 5, 80131 Naples, Italy

24 + **These authors contributed equally to the work**

25 ***Corresponding authors**

26 Francesco Prattichizzo, PhD

27 IRCCS MultiMedica

28 Via Fantoli 16/15 Milano, Italy

29 francesco.prattichizzo@multimedica.it

30

31 Jacopo Sabbatinelli, MD, PhD

32 Department of Clinical and Molecular Sciences, DISCLIMO, Università Politecnica delle Marche,

33 Via Tronto, 10/a Ancona, Italy

34 j.sabbatinelli@pm.univpm.it

35

36

37 **ABSTRACT**

38 Innovative biomarkers are needed to improve the management of patients with type 2 diabetes
39 mellitus (T2DM). Blood circulating miRNAs have been proposed as a potential tool to detect T2DM
40 complications but the lack of tissue specificity, among other reasons, has hampered their translation
41 to clinical settings. Extracellular vesicle (EV)-shuttled miRNAs have been proposed as an alternative
42 approach. Here, we adapted an immunomagnetic bead-based method to isolate plasma CD31 positive
43 (+) EVs to harvest vesicles deriving from tissues relevant for T2DM complications. Surface marker
44 characterization showed that CD31⁺ EVs were also positive for a range of markers typical of both
45 platelets and activated endothelial cells. After characterization, we quantified 11 candidate miRNAs
46 associated with vascular performance and shuttled by CD31⁺EVs in a large (n=218), cross-sectional
47 cohort of patients categorized as T2DM without complications, T2DM with complications, and
48 controls. We found that 10 of the tested miRNAs are affected by T2DM, while the signature
49 composed by miR-146a, -320a, -422a, -451a efficiently identified T2DM patients with complications.
50 Furthermore, another CD31⁺EV-shuttled miRNA signature, i.e. miR-155, -320a, -342-3p, -376, and
51 -422a, detected T2DM patients with a previous major adverse cardiovascular event. Many of these
52 miRNAs significantly correlate with clinical variables held to play a key role in the development of
53 complications. In addition, we show that CD31⁺ EVs from patients with T2DM are able to promote
54 the expression of selected inflammatory mRNAs, *i.e.* *CCL2*, *IL-1 α* , and *TNF α* , when administered to
55 endothelial cells *in vitro*. Overall, these data suggest that the miRNA cargo of plasma CD31⁺ EVs is
56 largely affected by T2DM and related complications, encouraging further research to explore the
57 diagnostic potential and the functional role of these alterations.

58

59 **Keywords:** extracellular vesicles; exosomes; CD31; microRNA; type 2 diabetes mellitus; T2DM
60 complications; cardiovascular diseases; MACE; low-grade inflammation.

61 INTRODUCTION

62 Type 2 diabetes mellitus (T2DM) is a chronic, heterogeneous disease caused by a multi-layer
63 interaction between the genetic makeup and environmental/lifestyle dependent factors (1). T2DM is
64 the cause of morbidity and mortality, mainly due to its cardiovascular (CV) complications, *e.g.*
65 ischemic heart disease and peripheral vascular disease (2). A number of additional alterations concur
66 to the development of CV complications in diabetic patients (1; 3). Given the complexity and
67 heterogeneity of the disease, many potential biomarkers for the development of CV diseases in T2DM
68 patients have been explored (4).

69 Blood circulating miRNAs have been proposed as a potential tool to improve CV risk assessment
70 among patients with T2DM and other conditions (5-7). Given plasma miRNA stability and their
71 ability to sense environmental stressors and modulate multiple pathways accordingly, miRNAs seem
72 to be the ideal candidates to provide useful information in complex and heterogeneous diseases like
73 T2DM complications and CV diseases in general (8; 9). However, at present, neither single miRNAs
74 nor miRNA signatures have been translated into clinical settings for diagnostic purposes. Many
75 reasons have hampered their use as biomarkers, including the lack of disease specificity and the
76 confounding effect provided by the relative contributions of different tissues to the plasma miRNA
77 pool (10; 11). To overcome these issues, the isolation of specific miRNA cargos, and in particular of
78 extracellular vesicles (EV)s, has been proposed (10; 12).

79 EVs are membrane-coated nanoparticles actively and/or passively released by almost all cell types.
80 EVs can be categorized according to a specific characteristic or by their size. Small EVs (diameter
81 <100 nanometres) derive from either multivesicular bodies or the plasma membrane, while larger
82 vesicles (between 100 nanometres and 1 micron) mostly derive from the plasma membrane (13). Both
83 EV types are able to shuttle and deliver functional nucleic acids, including miRNAs. Blood contains
84 a heterogeneous mixture of EVs of different origin, which are currently being characterized for
85 therapeutic and diagnostic purposes (14-16). In particular, recent evidence suggests a key role for
86 EV-shuttled miRNAs in the etiopathogenesis of both T2DM and its vascular complications (17-20).

87 However, few studies have quantified the miRNA payload of circulating EVs in relation to human
88 T2DM (21; 22), while only one study assessed EV-shuttled miRNAs in a setting of T2DM
89 complications (23). A recent paper showed that the majority of circulating EV-shuttled miRNAs
90 derive from the adipose tissue, a key organ for the development of T2DM (24). On the other side,
91 platelets, immune cells, and endothelial cells play a prominent role in the development of T2DM-
92 related complications (25; 26). Given the marked and specific expression of CD31, *i.e.* platelet
93 endothelial cell adhesion molecule (PECAM-1), in these three cell types, we adapted a previously
94 published immunomagnetic method (27) using commercially available beads to selectively capture
95 CD31 positive (+) EVs from plasma. After MISEV guidelines-driven characterization, we measured
96 a panel of 11 miRNAs previously associated with vascular performance in a cross-sectional cohort
97 of 218 subjects, categorized as healthy controls (Ctrl), patients with T2DM but without complications
98 (NC), and T2DM patients with complications (C). Here, we provide the first evidence of a specific
99 miRNA signature shuttled by CD31⁺EVs able to efficiently discriminate between T2DM patients
100 with complications from those without complications, and show that CD31⁺ EVs from patients with
101 T2DM are able to promote pro-inflammatory pathways when administered to endothelial cells *in*
102 *vitro*.

103

104 **RESEARCH DESIGN AND METHODS**

105 **Cohort description, plasma isolation, and sample size**

106 Samples derive from a previously published cohort composed of 501 patients with T2DM and 400
107 healthy control subjects (28). Informed consent was obtained from each subject and the study protocol
108 was approved by the local research ethics committee. T2DM was diagnosed according to the ADA
109 criteria (29). Inclusion criteria for patients with diabetes were BMI < 40 kg/m², age 35–85years,
110 ability and willingness to give written informed consent. Information collected included data on vital
111 signs, anthropometric factors, medical history, and behaviors. The presence/absence of diabetic
112 complications was evidenced as follows: diabetic retinopathy by fundoscopy through dilated pupils

113 and/or fluorescence angiography; nephropathy, defined as a urinary albumin excretion rate
114 $>30\text{mg}/24\text{h}$ and/or an estimated glomerular filtration rate (eGFR) $<60\text{ ml}/\text{min per } 1.73\text{m}^2$; neuropathy
115 established by electromyography; ischemic heart disease defined by clinical history, and/or ischemic
116 electrocardiographic alterations; peripheral vascular disease, including atherosclerosis obliterans and
117 cerebrovascular disease based on history, physical examinations, and Doppler velocimetry. Among
118 the 101 patients analyzed with T2DM and at least one complication, 28 had neuropathy, 22 peripheral
119 vascular disease, 20 nephropathy, 48 retinopathy and 52 major adverse cardiovascular events
120 (MACE). Healthy subjects were selected from a larger population of subjects belonging to a
121 prevention program (30). Concentrations of common analytes were measured by standard procedures.
122 As suggested by the MISEV initiative (65), fasting blood samples (collected in 4ml plasma EDTA
123 tubes) of all subjects were centrifuged at 753 g at 4°C to obtain platelet-poor EDTA plasma and stored
124 at -80°C within 3 hours from blood collection. Sample size was calculated based on our previous
125 publications (9; 31; 32).

126 **Isolation of CD31⁺ extracellular vesicles**

127 Plasma EDTA samples were allowed to thaw at room temperature. Appropriate volume (100 μl when
128 used for singular miRNA dosage, as indicated in the text for the other experiments) was diluted with
129 an equal amount of PBS. To remove apoptotic bodies and residual cellularity, sample were pre-
130 cleared by two subsequent centrifugations at 4°C , one at 2'000 g for 30 minutes and the following at
131 10'000 g for 45 minutes. Supernatant is diluted with PBS to reach 500 μl of volume and then mixed
132 with FcR Blocking Reagent (20 μl) provided in the commercially available kit for endothelial cells
133 isolation (130-091-935, Miltenyi Biotec). After vortexing, 20 μl of CD31 MicroBeads (130-091-935,
134 Miltenyi Biotec) are added to the suspension and incubated at 4°C in the dark for 30 minutes.
135 Appropriate (according to reaction volume) columns are mounted on the magnetic field and activated
136 with PBS. After incubation, the mixture is loaded onto the column to allow separation. After 3
137 washing with 500 μl of PBS, the column is removed from the magnetic support and CD31⁺EVs are
138 eluted in 500 μl PBS with the help of a plunger (**Figure 1A**). As a negative control, isotype control

139 beads (Dynabeads M-280) and no beads (equal amount of PBS) were used for parallel isolation of
140 EVs to test for eventual non-specific bindings of EVs and subjected to MACSPlex comparison
141 (methods below). We have submitted all relevant data of our experiments to the EV-TRACK
142 knowledgebase (EV-TRACK ID: EV200038) (33).

143 **Isolation of extracellular vesicles through ultracentrifugation**

144 For comparative experiments, an aliquot of 1 ml of plasma was pre-cleared as indicated above and
145 then the supernatant was diluted with PBS and subjected to ultracentrifugation at 120'000 g (4°C) in
146 an S110AT rotor in a Sorvall MX 150 ultracentrifuge (Thermo Scientific Inc) for 1,5 hours. Pellets
147 were resuspended in PBS and ultra-centrifuged again at 120'000 g for an additional 1,5 hours. The
148 final pellets were resuspended in 500 µl of PBS. In one case, the depleted fraction of the CD31
149 isolation method was collected and subjected to the same steps of ultracentrifugation to undergo
150 nanoparticle tracking analysis.

151 **Nanoparticle tracking analysis (NTA)**

152 CD31⁺EVs were isolated starting from 1 ml of plasma as described and resuspended in PBS. Size and
153 concentration of vesicles was determined using NanoSight LM10 equipment (Malvern Instruments
154 Ltd) using different dilutions (34) and with the following parameters: camera at 30 frames per second,
155 camera level at 16, temperature between 21–25 °C and video recording time 60 s. Three videos were
156 recorded for each sample and analyzed with NanoSight NTA 3.1 software. Data were expressed as
157 mean ± SD of the three videos.

158 **Transmission electron microscopy (TEM)**

159 To explore vesicles morphology with TEM, 30µl of CD31⁺EVs samples were diluted with PBS,
160 allowed to dry on top of Formvar carbon coated grids for 25min and contrasted with 2% uranyl acetate
161 for 2min. Preparations were observed in a JEOL 1010 100kV Electron Microscope.

162 **Western Blot**

163 For Western Blot experiments, CD31⁺ EVs were ultracentrifuged to allow PBS discharge and direct
164 application of lysis buffer to the EV pellet. The same was done with EVs isolated through

165 ultracentrifuge. EV lysates were prepared in RIPA buffer containing a protease inhibitor cocktail and
166 quantified using the Bradford method. Next, the lysates were subjected to SDS-PAGE and transferred
167 to nitrocellulose membranes (Whatman). Membranes were then incubated with the primary
168 antibodies overnight at 4°C. The following primary antibodies were used: CD31 (#3528, Cell
169 Signaling), Alix (#92880, Cell Signaling), TSG101 (ab125011, Abcam), CD63 (ab59479, Abcam),
170 ApoB100 (ab20737, Abcam), and ApoA1 (sc-30089, Santa Cruz Biotechnology). Fifty µg of whole
171 plasma proteins were also run as positive control for ApoA1. After incubation with the specific HRP-
172 conjugated antibody (Vector), proteins were detected by using enhanced chemiluminescence (ECL)
173 (GE Healthcare) and band densities were quantified by densitometry using ImageJ software.

174 **Cytofluorimetric detection of EV markers**

175 A commercially available (130-108-813, MACSPlex Exosome Kit, Miltenyi) and previously
176 validated (35) kit was used for cytofluorimetric detection of a large range of markers in isolated EVs.
177 Briefly, EVs isolated starting from the same amount of plasma were prepared as described in the
178 manufacturer protocol. The multiplex bead-based platform was analyzed by flow cytometry using a
179 BD FACSCantoII flow cytometer with the corresponding software (Becton, Dickinson and Company,
180 New Jersey, USA) equipped with a 488nm and a 640nm laser. Fluorescence emission was collected
181 by 530/30 nm, 585/42 nm, and 660/20 nm bandpass filters. At least 1'000 beads per sample were
182 examined and mean fluorescence intensity (MFI) was determined using BD FACSDiva 6.1 software.
183 Background signals were determined by analyzing beads incubated only with the respective staining
184 antibodies and subtracted from the signals obtained for beads incubated with EVs and stained with
185 the corresponding antibody. The Multiplex bead-based platform includes Setup Beads for flow
186 cytometer setup.

187 **RNA extraction and miRNA profiling**

188 Plasma samples from 4 subjects were pooled to reach 1 ml. CD31⁺EVs were isolated from 5 Ctrl
189 preparations and 5 T2DM preparations. RNA was extracted with a commercial kit known to enrich
190 small RNA species (Norgen Biotek Corporation). The same amount of RNA was converted to cDNA

191 by priming with a mixture of looped primers using the manufacturer's instructions (MegaPlex kit,
192 Applied Biosystem). Nine μ l of cDNA were used for mature miRNA profiling by a real-time PCR
193 instrument equipped with a 384-well reaction plate and human miRNA Array pool A containing 367
194 different human miRNA assays in addition to selected small nucleolar RNAs and negative controls
195 (non-human miRNAs). Only miRNAs expressed in more than one sample were included in the
196 analysis. 2^{-Ct} of the average values of each miRNA were used to build the heatmap comparing Ctrl
197 and T2DM with the ClustVis web tool (<https://biit.cs.ut.ee/clustvis/>) (36). Profiling raw data were
198 deposited in GEO and are accessible with the accession number GSE142553.

199 **Single miRNA quantitation**

200 For single miRNA quantification, CD31⁺EVs were isolated from 100 μ l of plasma. After mixing with
201 lysis buffer and before loading to the RNA separation column (Norgen), the synthetic *Caenorhabditis*
202 *elegans* miRNA, cel-miR-39, was spiked into plasma before RNA extraction. Only samples with cel-
203 miR-39 recovery > 95 % were used in subsequent analyses. Reverse transcription and miRNA
204 amplification were performed as previously described (9). Relative expression corresponded to the 2^{-
205 ΔCt value. Given the lack of an adequate endogenous control for plasma circulating miRNAs (11),
206 miRNA expression levels were generally normalized by cel-miR-39 levels, unless indicated
207 otherwise. To validate the 4-miRNA signature as a predictor of MACE in T2DM patients, global
208 mean normalization was performed for each miRNA by subtracting the mean of the Ct values of all
209 the miRNAs assessed in sample *i* from each individual Ct value from sample *i*. To compare the
210 diagnostic performance of CD31⁺EV-shuttled miRNAs with their whole plasma counterparts, we
211 used previously published data by our group for both miR-146a-5p (32) and miR-21-5p (9), extracting
212 the miRNA quantitation data for the same patients of this study. Previous data were generated using
213 the same amount of plasma, the same quantitation technology, and the same standardization method,
214 thus allowing data comparison through the relative receiver-operating characteristics (ROC) curves
215 as detailed below.

216 **EV fluorescent labelling, loading with cel-miR-39 or fluorescent small RNA, and treatment of**
217 **endothelial cells**

218 To use CD31⁺EVs for *in vitro* experiments, these were first detached from beads to avoid non-specific
219 toxicity and allow proper EV delivery to recipient cells. Briefly, EV/beads complexes (in 1.5 ml
220 tubes) were placed on the magnetic stand for 2 minutes. Then, PBS is removed and 300 µl of
221 EXOFLOW buffer (System Biosciences) were added. After incubation on a shaker at 25°C for 2
222 hours, samples are placed on the magnetic stand to remove the supernatant containing eluted EVs,
223 without disturbing the bead pellet. Collected EVs were quantified using NTA (data not shown).

224 As *in vitro* model of endothelial cells, human umbilical vein endothelial cells (HUVEC)s were used.
225 HUVECs were cultivated as previously described (38; 39). EV-depleted FBS (through overnight
226 centrifugation) was used for all the experiments. 1 x 10⁹ EVs were fluorescently labelled using
227 PKH67 membrane dye (Sigma-Aldrich). Labelled sEVs were washed in 10 ml PBS, collected by
228 ultracentrifugation, resuspended in PBS, and were then incubated with 50'000 recipient HUVECs for
229 24 h. HUVEC nuclei were counterstained with PBS-diluted 4',6-diamidino-2-phenylindole
230 dihydrochloride (DAPI, Sigma) for 15 minutes and cells were imaged at a widefield microscopy
231 (Axio Observer A1, Zeiss).

232 HUVECs were also treated for 24 h with EVs transfected with the non-human cel-miR-39 or with a
233 small fluorescent RNA. EVs were transfected with the Exo-Fect kit (System Biosciences) according
234 to the manufacturer's instructions. Briefly, EVs were prepared for transfection by combining Exo-
235 Fect solution, 20 pmol of cel-miR-39 (or the small fluorescent RNA), PBS and 1 x 10⁸ EVs. The
236 transfection solution was incubated at 37°C for 10 min and then put on ice. To stop the reaction, the
237 EXoQuick-TC reagent supplied in the kit was added. After centrifuging for 3 min at 140,000 rpm,
238 the supernatant was removed. The transfected EV pellet was suspended in 300 µl PBS and 150 µl of
239 transfected EVs were added to 50'000 HUVECs cultivated in 6 wells. The same amounts of cel-miR-
240 39 and Exo-Fect reagent were used as negative control.

241 To assess the pro-inflammatory effect of EVs, CD31+EVs were isolated from 1 ml of plasma from
242 Ctrl, T2DM-NC, or T2DM-C, detached from beads, and used to treat 50'000 HUVECs cultivated in
243 6 wells for 24 hours. Messenger RNA measurement by RT-PCR was performed as previously
244 described (38). Primers used were as previously reported (39).

245 **Statistical analysis**

246 Continuous variables were tested for normality using the Shapiro Wilk's test and reported as mean \pm
247 SD. To compare the expression of CD31+ EV-shuttled miRNAs in the three different groups, Kruskal-
248 Wallis followed by Dunn post hoc test was used, while to compare data from controls and T2DM
249 patients Mann-Whitney U test was applied. Categorical variables were compared using the Chi-
250 Squared test. Pearson's correlation was used to assess correlations between continuous variables.
251 One-way ANCOVA was used to evaluate differences in continuous variables between groups while
252 controlling for selected clinical and biochemical variables.

253 Multinomial logistic regression models were constructed to identify factors associated with the
254 diagnosis of T2DM and its complications. A parsimonious backward-stepwise elimination of non-
255 significant variables was deemed as appropriate in our setting. Model fit was assessed using the
256 Hosmer-Lemeshow goodness-of-fit test. The proportion of variance explained by the final model was
257 determined using the Nagelkerke R² statistic.

258 ROC curves were constructed for the single miRNAs and for the predicted probabilities derived from
259 the logistic regression models. The Youden's index was used to calculate the best cut-off values,
260 where appropriate. Multiple ROC curves were compared using the DeLong method (41).

261 The analyses were carried out using IBM SPSS Statistics, version 26 (IBM Corp, Armonk, NY, USA)
262 and R, version 3.6.1. Statistical significance was defined as a two-tailed p-value <0.05.

263 **Data and Resource Availability**

264 Profiling raw data were deposited in GEO and are available with the accession number GSE142553.

265 Data relative to EV isolation and characterization have been submitted to the EV-TRACK

266 knowledgebase (EV-TRACK ID: EV200038). All the other data generated during and/or analyzed
267 during the current study are available from the corresponding author upon reasonable request.

268 **RESULTS**

269 **Isolation and characterization of CD31⁺ extracellular vesicles**

270 After immunomagnetic capture from 1 ml of pooled plasma samples from control subjects (**Figure**
271 **1A**, details in methods), standard nanoparticles tracking analysis (NTA) was used to quantify our EV
272 isolate. NTA revealed that our method is able to mostly isolate vesicles compatible with the size of
273 small EVs (14) (**Figure 1B**). Isolated EVs were also characterized by TEM, which showed round-
274 shaped vesicles with a minimal presence of contaminants (**Figure 1C**). To further characterize the
275 collected EV population and to control their positivity for CD31, we compared this method with a
276 standard approach to isolate EVs, *i.e.* ultracentrifugation (UC, at 120'000 g). We subjected EVs
277 isolated from 1 ml of plasma to comparative analysis (from the same pooled control samples, n=6)
278 for both Western Blot and surface markers expression with a specific kit to detect EV proteins through
279 cytofluorimeter (35). As suggested by MISEV guidelines (14), EVs collected with CD31 beads were
280 positive for EV-associated transmembrane, *i.e.* CD63 and CD31, and cytosolic, *i.e.* Alix and TSG101,
281 proteins (**Figure 1D**). In addition, the CD31-beads method enriched the population of CD31+EVs
282 compared to UC, as demonstrated by a higher ratio of CD31 over conventional EV markers. In
283 addition, since lipoproteins are often isolated as contaminants with various EV isolation methods, we
284 tested the expression of ApoA1 and ApoB100, two major components of lipoproteins. Albeit positive
285 with both CD31 beads and UC, the immunomagnetic method was accompanied by a lower presence
286 of these contaminants (**Figure 1D**). To substantiate these findings, the same comparison was
287 subjected to cytofluorimetric detection of the EV markers CD9, CD63, and CD81, as well as of CD31.
288 As expected, the CD31-beads method enriched the population of CD31⁺EVs compared to UC, as
289 demonstrated by an increased ratio of CD31 over EV surface markers in CD31⁺ EVs compared to
290 EVs isolated with UC (**Figure 1E**). To explore whether the use of beads for isolation is associated
291 with a non-specific binding of EVs and to gain preliminary insights into the putative cell source of

292 CD31⁺ EVs, we compared EVs isolated through CD31 beads to those eventually collected using
293 beads with isotype control or using no beads, starting from the same amount of volume (1 ml, n=3)
294 and using the same procedure. Cytofluorimetric detection of a large range of surface markers revealed
295 a significantly higher expression of EV markers, but also of a large range of epitopes typical of
296 platelets, *i.e.* CD41b and CD42a, and activated endothelial cells, *i.e.* CD62P. However, also CD49e,
297 CD29, and CD69 (beyond tetraspanins) were significantly increased with CD31 beads. (**Figure 1F**).
298 Indeed, all the other tested markers (35) were not expressed in our EVs (data not shown). To explore
299 which fraction of total plasma EVs is represented by the isolated EVs, we collected the depleted
300 fraction of the CD31 beads method and, after UC, subjected it to NTA comparison (control samples;
301 n=3), which revealed that the concentration of collected CD31⁺ EVs is significantly lower than its
302 depleted counterpart (**Figure 1G**). In addition, we compared the surface markers expression of
303 CD31⁺EVs vs the CD31 depleted fraction. Results evidenced a higher abundance of the platelets
304 marker CD41b and a lower positivity for common EVs markers, *i.e.* CD9, CD63, and CD81 in
305 CD31⁺EVs compared with the depleted fraction (**Supplementary Figure 1A**). To explore the yield
306 efficiency of our isolation technique, we compared the abundance of CD31 in UC-isolated EVs, in
307 isolated CD31⁺EVs, and in the CD31 depleted fraction starting from the same samples processed in
308 succession. We found no significant differences in the abundance of CD31 between the initial sample
309 and CD31⁺EVs, while a significant decrease was observed in the CD31 depleted fraction compared
310 with the initial sample (**Supplementary Figure 1B**). To test whether isolating CD31⁺ EVs yields
311 quantitatively different results in terms of miRNA abundance compared to UC and to whole plasma
312 (42; 43), the same amount of plasma was used for the isolation of CD31⁺EVs, EVs with UC, or left
313 untreated (except for pre-clearance) and then these three samples were subjected to RNA extraction
314 to quantify four miRNAs commonly studied in settings of T2DM and CVD, *i.e.* miR-126-3p, miR-
315 146a-5p, miR-155, and miR-21-5p (10). All miRNAs were consistently expressed with the three
316 tested approaches, being higher in total plasma, followed by EVs isolated through UC, and finally in
317 CD31⁺EVs (**Figure 1H**), in line with the observation that CD31⁺EVs represent only a fraction of

318 total plasma EVs. Overall, these data suggest that our isolation method harvests CD31⁺ EVs,
319 representing a fraction of plasma EVs with a heterogenous origin but compatible with the hypothesis
320 that platelets and endothelial cells contribute to this specific EVs pool.

321

322 **Comparative concentration, size and miRNA profiling of CD31⁺ EVs from controls and** 323 **patients with T2DM**

324 To explore if T2DM affects the number and size of CD31⁺ EVs, we compared four pooled samples
325 from healthy controls with four pooled samples from patients with T2DM without complications (1ml
326 each). NTA showed that the concentration of CD31⁺ EVs was not significantly affected by T2DM
327 (**Figure 2A**), while a slight but significant decrease in their modal size was also observed (**Figure**
328 **2B**). Cytofluorimetric comparison of surface markers supported NTA data, since the expression of
329 CD31, CD9, CD63, and CD81 was also slightly but not significantly increased in T2DM samples
330 (n=4) (**Figure 2C**).

331 Then, we performed a comparative profiling of miRNA content within CD31⁺EVs comparing Ctrl
332 and T2DM patients (5 vs 5 samples with each sample prepared from pooled plasma). Of the 367
333 profiled miRNAs, 103 were detectable in at least one sample (**Figure 2D**), and 39 were expressed in
334 4 out of 5 (80%) of the tested samples. Comparison of Ctrl and T2DM evidenced a different relative
335 quantity of miRNAs in CD31⁺EVs (**Figure 2D**).

336

337 **Diagnostic performance of a selected miRNA signature for T2DM status and complications**

338 To explore the possible association of CD31⁺EV-shuttled miRNAs with T2DM status and T2DM
339 complications, we selected 11 miRNAs for two characteristics: 1. being proposed to play a role in the
340 development of CV complications of T2DM or previously suggested to have diagnostic potential in
341 CV studies (**Supplementary Table 1** for supporting literature) and 2. being robustly expressed in our
342 setting of isolated CD31⁺ EVs (**Figure 2B**). This selected panel was composed of miR-126-3p, miR-
343 146a-5p, miR-155, miR-195-5p, miR-21-5p, miR-24-3p, miR-320a, miR-342-3p, miR-376a, miR-

344 422, and miR-451a. We quantified single miRNAs by qPCR in CD31⁺ EVs isolated from plasma of
345 a cross-sectional cohort of 218 individuals, including 60 healthy (Ctrl), 57 with uncomplicated T2DM
346 (T2DM-NC), and 101 with T2DM and complications (T2DM-C). The clinical, anthropometrical, and
347 biochemical variables of the subjects are reported in **Table 1**.

348 Analysis of the expression profiles among groups revealed significant differences for all the evaluated
349 miRNAs, except miR-376a. **Supplementary Table 2** reports the relative expressions of the 11
350 miRNAs in each group, along with the results of the Student's *t* (CTR vs. T2DM) and one-way
351 ANOVA (CTR vs. T2DM-NC vs. T2DM-C) tests, while **Figure 3** shows boxplots of the miRNA
352 expression values across groups. Specifically, the circulating levels of 5 miRNAs, *i.e.* miR-21-5p, -
353 146a, -342-3p, -422a, and -451a, are increased in T2DM patients, while 5 miRNAs, *i.e.* miR-24-3p,
354 -126-3p, -155, -195-5p, and -320a, show decreased levels in T2DM. The post-hoc comparisons
355 between the T2DM-NC and T2DM-C groups revealed significant differences for miR-21-5p, -146a,
356 -342-3p, -422a and -451a (increased in T2DM-C); and for miR-320a (decreased in T2DM-C).

357 Therefore, ROC curves were generated to evaluate the diagnostic potential of these 10 miRNAs in
358 detecting T2DM. Analysis of the ROC curves, showed in **Figure 4A**, revealed an outstanding
359 diagnostic accuracy ($AUC \geq 0.90$) for 5 miRNAs (list), and an excellent accuracy ($0.80 \leq AUC <$
360 0.90) for 3 miRNAs (list). A second set of ROC curves was generated to assess the ability of the 6
361 miRNAs differentially regulated in T2DM-C vs. T2DM-NC to discriminate between the two groups.
362 The diagnostic accuracy was acceptable for all of the 6 miRNAs, with AUCs ranging from 0.67 (miR-
363 146a) to 0.80 (miR-342-3p) (**Figure 4B**).

364 To test whether harvesting CD31⁺ EVs increases the ability of selected plasma miRNAs to detect
365 T2DM and its complications, we compared the diagnostic performance of miR-146a-5p and miR-21-
366 5p shuttled in CD31⁺ EVs with those of the same miRNAs quantified in the same amount of whole
367 plasma. ROC curves indicate that CD31⁺EV-shuttled miR-146a-5p and miR-21-5p have a higher
368 performance to detect both T2DM (AUC 0.911 vs 0.562, $p < 0.0001$; and 0.859 vs 0.595, $p < 0.0001$;
369 respectively) (**Figure 4C**) and T2DM complications (AUC 0.673 vs 0.533, $p = 0.028$; and 0.744 vs

370 0.511, $p < 0.001$; respectively) compared to their whole plasma counterparts (**Figure 4D**), suggesting
371 that the isolation of CD31+ EVs improve the diagnostic potential of plasma miR-146a-5p and miR-
372 21-5p.

373 **Diagnostic performance of the minimum miRNA signature for T2DM complications and major** 374 **adverse cardiovascular events**

375 To obtain the smallest possible signature with the highest discriminatory power for T2DM
376 complications, we built a binary logistic regression to ascertain the effects of the 11 miRNAs,
377 expressed as Z-scores, on the likelihood of complications in T2DM patients, with a backward
378 stepwise procedure to achieve the most parsimonious model. The logistic regression model was
379 statistically significant ($\chi^2(4) = 58.611$, $p < 0.001$) and explained 42.5% (Nagelkerke R^2) of the
380 variance. Four miRNAs were retained into the model as significant predictors, *i.e.* miR-146a, -320a,
381 -422a, -451a (**Supplementary Table 3**). A similar model was built including BMI and LDL-C as
382 covariates, since these variables were not balanced between groups. As shown in **Supplementary**
383 **Table 4**, inclusion of these covariates marginally affected the results.

384 Next, we tested the association between the 4-miRNA signature and the risk of MACE in T2DM
385 patients. After inclusion in the model of HbA1c and the common risk factors age, gender, LDL-C,
386 and hypertension as covariates, we still observed a strong association ($p < 0.001$) between our
387 signature and history of MACE. This logistic regression model was statistically significant ($\chi^2(6) =$
388 102.960 , $p < 0.001$) and explained 66.7% of the variance (**Table 2**). To test whether this signature
389 remains significant using a different normalization method (11), an additional logistic regression
390 model was built after recalculating the signature using the global-mean (derived from all the
391 quantified miRNAs)-normalized expression of 4 miRNAs. The regression model proved statistically
392 significant ($\chi^2(6) = 86.572$, $p < 0.001$, $R^2 = 0.587$) and included the 4-miRNA signature ($p < 0.001$),
393 increasing HbA1c ($p = 0.031$) and male gender ($p = 0.044$) as significant predictors of MACE (**Table**
394 **2**).

395 To assess whether other CD31⁺EV-shuttled miRNA signatures are associated to the development of
396 MACE in T2DM patients, we built an additional logistic regression model with backward selection
397 on the 11 miRNAs, including age, gender, LDL-C, HbA1c, and hypertension as covariates. Again,
398 the logistic regression model was statistically significant ($\chi^2(7) = 155.777$, $p < 0.001$) and explained
399 87.3% of the variance. Of the 7 miRNAs which were retained into the model as predictors, 5 were
400 statistically significant, *i.e.* miR-155, -320a, -342-3p, -376, and -422a. **Table 2** summarizes the model
401 and shows the adjusted odds ratios (OR) for each miRNA.

402 To assess whether CD31⁺EV-shuttled miRNAs associate with other complications of T2DM,
403 multiple one-way ANCOVAs were computed to explore the relationship between the 11 miRNAs
404 and T2DM complications after adjusting for age and gender. **Supplementary Table 5** reports the
405 adjusted means for each miRNA in subjects with or without a specific complication. We observed a
406 significant differential regulation of all the CD31⁺EV-shuttled miRNAs, except miR-126, in
407 macrovascular complications, *i.e.* peripheral artery disease and MACE. The association between the
408 levels of 9 miRNAs and MACE remained significant even after adjustment for HbA1c and the
409 presence of other concomitant T2DM complications. On the contrary, no significant association was
410 found between miRNAs and any of the microvascular complications. Since blood miRNAs and
411 especially platelet derived miRNAs have been shown to be affected by anti-platelet therapies (47),
412 we explored whether anti-platelet medications affected our results. However, we did not observe any
413 significant effect of anti-platelet therapy on miRNA expression (data not shown).

414 **Correlations with clinical variables and between miRNAs**

415 We then explored the association between the 11 CD31⁺EV-shuttled miRNAs and a large range of
416 relevant biochemical and clinical variables. The resulting color-coded correlation plot is shown in
417 **Figure 5A**. The correlation coefficient ranged from -0.51 to 0.40. A similar correlation plot was
418 drawn to highlight reciprocal correlations between the levels of the 11 miRNAs under investigation
419 (**Figure 5B**). The complete correlation matrix is reported in **Supplementary Table 6**. Notably, the
420 levels of all the T2DM-associated miRNAs, except miR-320a, are linearly related with fasting

421 glucose and, among these, 7 miRNAs correlate also with HbA1c, whereas only 2 miRNAs correlate
422 with homeostatic model assessment-insulin resistance (HOMA-IR). While our miRNA signature
423 showed no significant association with the presence of diabetic nephropathy, 9 miRNAs are linearly
424 related to either serum creatinine, azotemia, or eGFR, with the direction of the correlation being
425 concordant with the expected deterioration of the renal function with worsening glycemic control.
426 Eight miRNAs showed an association with age, with 6 miRNAs also being inversely correlated with
427 PBMC telomere length. In addition, we observed a remarkable pattern of correlations between 8
428 miRNAs and the lipid profile. Of note, 7 out of 8 of these miRNAs showed also a correlation with
429 waist/hip ratio, fasting glucose, and HbA1c with an inverse trend when compared to their correlation
430 with lipid profile, suggesting a divergent effect of common CV risk factors on these variables.
431 Overall, these data indicate that CD31⁺EV-shuttled miRNAs may sense a wide range of common risk
432 factors known to be key drivers of T2DM complications development. Finally, many of the miRNAs
433 were significantly associated with one another (**Figure 5B**), extending the knowledge that circulating
434 miRNAs are highly correlated also to those shuttled by CD31⁺EVs (11).

435 **CD31⁺ EVs from patients with T2DM promote inflammation in endothelial cells *in vitro***

436 To explore whether the altered miRNA cargo of CD31⁺ EVs derived from patients with T2DM affects
437 the functional properties of these EVs when administered *in vitro* to endothelial cells, we unbound
438 collected EVs from beads with a commercially available buffer and the help of a magnet (**Figure 6A**,
439 details in methods). First, we verified the ability of endothelial cells to uptake EVs stained with a
440 fluorescent dye after a 24h incubation (**Figure 6B**, representative image of a n = 3 EVs preparation
441 from control samples). Since fluorescent dyes might be accompanied by non-specific binding to the
442 lipidic components of the cells (64), we loaded a small RNA with a red fluorophore into EVs and
443 then used them to treat endothelial cells. We detected a consistent red fluorescence in recipient cells,
444 suggesting that collected EVs were able to deliver small RNAs to recipient endothelial cells (**Figure**
445 **6C**). To support this observation, we administer EVs transfected with a non-human miRNA, *i.e.* cel-
446 miR-39, to endothelial cells (n=3, EVs isolated from control samples). The same amount of EV-free,

447 cel-miR-39 (along with the transfecting reagent), PBS, and non-transfected EVs were used as
448 negative controls. As shown in **Figure 6D**, cel-miR-39 expression was higher in endothelial cells
449 treated with transfected EVs compared to the same amount of this miRNA not loaded onto EVs, while
450 cel-miR-39 was undetectable in the other two negative controls (data not shown). Given that many
451 of the CD31⁺ EV miRNAs found to be altered by T2DM and its complications (**Figure 3**) have been
452 previously associated with the alteration of inflammatory pathways (16; 25), we treated endothelial
453 cells with CD31⁺ EVs derived from control, T2DM-NC, and T2DM-C (n=3 each, from 1 ml of
454 plasma) and measured the expression of a panel of pro-inflammatory genes at the mRNA level. EVs
455 from both T2DM-NC and T2DM-C significantly increased the expression of chemokine (C-C motif)
456 ligand 2 (*CCL2*, also referred to as monocyte chemoattractant protein-1, *i.e.* *MCP-1*) and interleukin
457 1 α (*IL-1 α*) when compared to EVs from control subjects, while only EVs from T2DM-C induced the
458 expression of *TNF α* in recipient endothelial cells when compared to both T2DM-NC and controls.
459 Finally, the expression of *IL-6*, chemokine (C-X-C motif) ligand (*CXCL*)-1, and *CXCL-8* was not
460 affected by any of the treatments (**Figure 6E**), possibly suggesting a peculiar pro-inflammatory effect
461 of EVs, rather than a non-specific inflammatory response.

462 **DISCUSSION**

463 Circulating miRNA quantification has already been proposed as a potential approach to evaluate CV
464 risk (47-49). However, while data on circulating miRNAs in the setting of CV diagnostic for the
465 general population are promising (47), none of the miRNAs has been translated into the clinic for
466 diagnostic purposes, including in the context of T2DM-related complications. Lack of standardization
467 methods and the complex contribution of different tissues and pathological processes to circulating
468 miRNA pool are among the reasons that limit their use (10; 11). To overcome these issues, the
469 quantification in specific miRNA cargos has been proposed. Indeed, microvesicle (MV)-shuttled
470 miR-126 and miR-199a but not freely circulating miRNA expression predict the occurrence of CV
471 events in patients with stable coronary artery disease (18), while T2DM patients with prevalent CVD
472 show low miR-26a and miR-126 levels within large MVs (50). In particular, it was suggested that

473 MV-shuttled miRNAs derive from endothelial cells (18; 51), while the most abundant miRNAs in
474 whole plasma are among those highly expressed in platelets (7; 44; 52). However, since a seminal
475 paper indicated that the majority of exosomal (*i.e.* small EVs) miRNAs derive from adipose tissue
476 (24), we decided to harvest EVs expressing CD31, in order to enrich EVs derived from platelets,
477 endothelial cells, and immune cells, *i.e.* the most relevant cellular components in the etiopathogenesis
478 of T2DM complications. We showed here that the isolation of CD31⁺ EVs results in a EVs pool
479 compatible with a platelet and endothelial cell origin, as shown by analysis of surface markers
480 expression. However, since also other markers were positive, the origin of collected EVs is likely
481 heterogenous.

482 A recent study has characterized the abundance and functional alterations of circulating EVs from
483 patients with T2DM, showing a higher plasma EV concentration in individuals with diabetes, an
484 observation obtained by isolating EVs with both a commercial kit and UC (53). However, when
485 comparing surface marker expression, erythrocyte-derived EVs were significantly increased by
486 T2DM, while a non-significant trend was observed for platelets/endothelial cells derived particles
487 (53), an observation compatible with our results. In addition, the same study showed that EVs from
488 patients with T2DM are able to induce an inflammatory response in recipient monocytes *in vitro*.
489 Another study found that also EVs from patients with gestational diabetes promote inflammation
490 when administered to endothelial cells (55). Here, we extend these findings by showing that also
491 CD31⁺ EVs from patients with T2DM are able to foster low-grade inflammation in recipient
492 endothelial cells, with a variable effect when considering T2DM with or without complications.
493 Given that EVs can shuttle a large repertoire of molecules, research aimed at studying the specific
494 components fostering inflammatory pathways might provide useful information for the
495 etiopathogenesis of the disease, especially considering that low-grade inflammation is associated with
496 the presence of T2DM complications (56). To our knowledge, only one study used the CD31 beads
497 approach to isolate EVs from patients with T2DM (57). In that study, CD31⁺ EVs were shown to

498 boost apoptosis resistance of vascular smooth muscle cells cultured in hyperglycaemic condition, an
499 effect possibly mediated by membrane-bound platelet-derived growth factor-BB.

500 Few studies quantified miRNA abundance within EVs in diabetic cohorts (21; 22; 58; 48,50).
501 Interestingly, two studies found an increased abundance of miR-126-3p in EVs from T2DM patients
502 (22; 23), while here a slightly decreasing trend was observed for CD31⁺EV-shuttled miR-126-3p.
503 This miRNA was previously suggested as one of the most downregulated miRNAs when analysing
504 whole plasma or large endothelial MVs (9; 18; 59). On the contrary, miR-21-5p in CD31⁺EVs showed
505 an opposite trend compared to the previously observed decrease in plasma of T2DM patients, but not
506 in total EVs (9; 59). Assuming that CD31⁺ EVs derive mainly from platelets and endothelial cells,
507 our results might appear consistent with the observation that hyperglycaemia induced a
508 downregulation of mir-126-3p in endothelial EVs (18) and in platelets (60). The two studies finding
509 an increased expression of miR-126-3p (22; 23) were performed using different isolation methods
510 that collect a broader EV population, possibly suggesting that the effect of T2DM on miR-126-3p
511 expression is divergent when considering different tissues. Indeed, two different mouse models of
512 insulin resistance showed an increased expression of miR-126-3p in the liver (61) and in the adipose
513 tissue (62). Considering also that the majority of plasma EV miRNAs are held to derive from adipose
514 tissue (24), it is conceivable that a broad, non-tissue specific EVs collection method provides opposite
515 results if compared with an immunomagnetic method likely enriching for tissue-specific EVs. On
516 the other side, miR-21-5p shuttled in total EVs is increased in T2DM patients with diabetic
517 nephropathy compared to non-complicated patients (23), similarly to our observation when
518 considering CD31⁺ EVs-shuttled miR-21-5p and T2DM complications as a whole. Notably, even
519 though miR-21-5p shuttled in CD31⁺ EVs was not associated with prevalent nephropathy in our
520 cohort, its levels were correlated with multiple measures of kidney function. All these observations
521 suggest that harvesting rare EV fractions or subpopulations might hold an increased potential for
522 miRNA-biomarker discovery if compared to broader EV collections or to whole plasma, possibly
523 limiting the heterogeneous, pleiotropic effect of T2DM on the expression of miRNAs at the tissue

524 level. The results showing an increased performance of CD31⁺EV-shuttled miR-21-5p and miR-
525 146a-5p compared to the whole plasma levels of the same miRNAs in detecting both T2DM and its
526 complications might support this hypothesis.

527 **Limitations of the study**

528 The main limitation of this study is that we used a cross-sectional cohort, thus we cannot determine
529 if the obtained signature is able to longitudinally identify patients at risk of T2DM complications or
530 specifically MACE. Moreover, given this study design, we cannot perform a direct comparison with
531 already available tools. In addition, the BMI of patients with T2DM was significantly higher
532 compared to controls. However, since we isolated a specific fraction of EVs, the concentration of
533 which was not affected by T2DM, it is unlikely that the observed differences in miRNA abundance
534 are solely ascribable to the diverse quantity of adipose tissue between T2DM patients and controls.
535 In addition, plasma isolation was performed with a low centrifugation speed, which might have left
536 residual platelets in the samples that could have been then activated by thawing. However, before
537 magnetic isolation, samples were precleared with two subsequent centrifugations, thus minimizing
538 the risk of a consistent contamination by platelets granules or fragments. Finally, we did not perform
539 functional experiments to explore which components of the EV-cargo are responsible of the observed
540 pro-inflammatory effect.

541 **Conclusions**

542 In summary, we have here isolated CD31⁺EVs in a large cohort of T2DM patients showing that
543 specific miRNA signatures associate with T2DM complications as a whole or individually with
544 MACE. We also show that harvesting CD31⁺ EVs, compared to whole plasma, improves the ability
545 of miR-21-5p and miR-146a-5p to detect T2DM and its complications. Finally, we also demonstrated
546 that CD31⁺ EVs from T2DM patients are endowed with pro-inflammatory properties when
547 administered *in vitro* to endothelial cells, overall encouraging further research to explore both the
548 diagnostic potential and the functional role of T2DM-driven EV alterations.

549

550

551 **ACKNOWLEDGMENTS**552 **Author Contributions**

553 F.P., F.O., and A.C. conceived the idea and designed the study. V.d.N. performed the majority of
554 experiments. J.S. and A.G. performed statistical analysis and prepared figures and tables. R.S. and E.
555 M. performed miRNA profiling and Western Blot experiments. C.C., M.P, and I.C. performed
556 cytofluorimeter and TEM experiments. A.G., N.B., M.R.R., A.R.B., L.L.S., A.D.P., S.G., G.M., A.N,
557 and P.d.C revised the paper for intellectual content and provided additional expertise. F.P., J.S, F.O.,
558 and A.C wrote the paper. The final version of the manuscript was approved by all authors.

559 F.P. is the guarantor of this work and, as such, had full access to all the data in the study and takes
560 responsibility for the integrity of the data and the accuracy of the data analysis.

561 **Conflict of interest**

562 None of the authors have competing interests.

563

564 **Sources of funding**

565 This work was supported by grants from La Maratò de TV3 to A.C and by the Italian Ministry of
566 Health (Ricerca Corrente) to IRCCS MultiMedica.

567

568

569

570 **REFERENCES**

- 571 1. DeFronzo RA, Ferrannini E, Groop L, Henry RR, Herman WH, Holst JJ, Hu FB, Kahn CR, Raz I, Shulman
572 GI, Simonson DC, Testa MA, Weiss R: Type 2 diabetes mellitus. *Nat Rev Dis Primers* 2015;1:15019
- 573 2. Dal Canto E, Ceriello A, Ryden L, Ferrini M, Hansen TB, Schnell O, Standl E, Beulens JW: Diabetes as a
574 cardiovascular risk factor: An overview of global trends of macro and micro vascular complications. *Eur J*
575 *Prev Cardiol* 2019;26:25-32
- 576 3. Gaede P, Lund-Andersen H, Parving HH, Pedersen O: Effect of a multifactorial intervention on mortality
577 in type 2 diabetes. *N Engl J Med* 2008;358:580-591
- 578 4. Bachmann KN, Wang TJ: Biomarkers of cardiovascular disease: contributions to risk prediction in
579 individuals with diabetes. *Diabetologia* 2018;61:987-995
- 580 5. Willeit P, Skrobilin P, Moschen AR, Yin X, Kaudewitz D, Zampetaki A, Barwari T, Whitehead M, Ramirez
581 CM, Goedeke L, Rotllan N, Bonora E, Hughes AD, Santer P, Fernandez-Hernando C, Tilg H, Willeit J, Kiechl
582 S, Mayr M: Circulating MicroRNA-122 Is Associated With the Risk of New-Onset Metabolic Syndrome and
583 Type 2 Diabetes. *Diabetes* 2017;66:347-357
- 584 6. Zampetaki A, Mayr M: Sweet dicer: impairment of micro-RNA processing by diabetes. *Circ Res*
585 2015;117:116-118
- 586 7. Mayr M, Zampetaki A, Kiechl S: MicroRNA biomarkers for failing hearts? *Eur Heart J* 2013;34:2782-2783
- 587 8. Zampetaki A, Willeit P, Drozdov I, Kiechl S, Mayr M: Profiling of circulating microRNAs: from single
588 biomarkers to re-wired networks. *Cardiovasc Res* 2012;93:555-562
- 589 9. Olivieri F, Spazzafumo L, Bonafe M, Recchioni R, Prattichizzo F, Marcheselli F, Micolucci L, Mensa E,
590 Giuliani A, Santini G, Gobbi M, Lazzarini R, Boemi M, Testa R, Antonicelli R, Procopio AD, Bonfigli AR:
591 MiR-21-5p and miR-126a-3p levels in plasma and circulating angiogenic cells: relationship with type 2
592 diabetes complications. *Oncotarget* 2015;6:35372-35382
- 593 10. Prattichizzo F, Giuliani A, De Nigris V, Pujadas G, Ceka A, La Sala L, Genovese S, Testa R, Procopio
594 AD, Olivieri F, Ceriello A: Extracellular microRNAs and endothelial hyperglycaemic memory: a therapeutic
595 opportunity? *Diabetes Obes Metab* 2016;18:855-867
- 596 11. Sunderland N, Skrobilin P, Barwari T, Huntley RP, Lu R, Joshi A, Lovering RC, Mayr M: MicroRNA
597 Biomarkers and Platelet Reactivity: The Clot Thickens. *Circ Res* 2017;120:418-435
- 598 12. Coumans FAW, Brisson AR, Buzas EI, Dignat-George F, Drees EEE, El-Andaloussi S, Emanuelli C,
599 Gasecka A, Hendrix A, Hill AF, Lacroix R, Lee Y, van Leeuwen TG, Mackman N, Mager I, Nolan JP, van
600 der Pol E, Pegtel DM, Sahoo S, Siljander PRM, Sturk G, de Wever O, Nieuwland R: Methodological
601 Guidelines to Study Extracellular Vesicles. *Circ Res* 2017;120:1632-1648
- 602 13. Witwer KW, Thery C: Extracellular vesicles or exosomes? On primacy, precision, and popularity
603 influencing a choice of nomenclature. *J Extracell Vesicles* 2019;8:1648167
- 604 14. Thery C, Witwer KW, Aikawa E, Alcaraz MJ, Anderson JD, Andriantsitohaina R, Antoniou A, Arab T,
605 Archer F, Atkin-Smith GK, Ayre DC, Bach JM, Bachurski D, Baharvand H, Balaj L, Baldacchino S, Bauer
606 NN, Baxter AA, Bebawy M, Beckham C, Bedina Zavec A, Benmoussa A, Berardi AC, Bergese P, Bielska E,
607 Blenkiron C, Bobis-Wozowicz S, Boilard E, Boireau W, Bongiovanni A, Borrás FE, Bosch S, Boulanger CM,
608 Breakefield X, Breglio AM, Brennan MA, Brigstock DR, Brisson A, Broekman ML, Bromberg JF, Bryl-
609 Gorecka P, Buch S, Buck AH, Burger D, Busatto S, Buschmann D, Bussolati B, Buzas EI, Byrd JB, Camussi
610 G, Carter DR, Caruso S, Chamley LW, Chang YT, Chen C, Chen S, Cheng L, Chin AR, Clayton A, Clerici
611 SP, Cocks A, Cocucci E, Coffey RJ, Cordeiro-da-Silva A, Couch Y, Coumans FA, Coyle B, Crescitelli R,
612 Criado MF, D'Souza-Schorey C, Das S, Datta Chaudhuri A, de Candia P, De Santana EF, De Wever O, Del
613 Portillo HA, Demaret T, Deville S, Devitt A, Dhondt B, Di Vizio D, Dieterich LC, Dolo V, Dominguez Rubio

- 614 AP, Dominici M, Dourado MR, Driedonks TA, Duarte FV, Duncan HM, Eichenberger RM, Ekstrom K, El
615 Andaloussi S, Elie-Caille C, Erdbrugger U, Falcon-Perez JM, Fatima F, Fish JE, Flores-Bellver M, Forsonits
616 A, Frelet-Barrand A, Fricke F, Fuhrmann G, Gabrielsson S, Gamez-Valero A, Gardiner C, Gartner K, Gaudin
617 R, Gho YS, Giebel B, Gilbert C, Gimona M, Giusti I, Goberdhan DC, Gorgens A, Gorski SM, Greening DW,
618 Gross JC, Gualerzi A, Gupta GN, Gustafson D, Handberg A, Haraszti RA, Harrison P, Hegyesi H, Hendrix A,
619 Hill AF, Hochberg FH, Hoffmann KF, Holder B, Holthofer H, Hosseinkhani B, Hu G, Huang Y, Huber V,
620 Hunt S, Ibrahim AG, Ikezu T, Inal JM, Isin M, Ivanova A, Jackson HK, Jacobsen S, Jay SM, Jayachandran
621 M, Jenster G, Jiang L, Johnson SM, Jones JC, Jong A, Jovanovic-Talisman T, Jung S, Kalluri R, Kano SI,
622 Kaur S, Kawamura Y, Keller ET, Khamari D, Khomyakova E, Khvorova A, Kierulf P, Kim KP, Kislinger T,
623 Klingeborn M, Klinke DJ, 2nd, Kornek M, Kosanovic MM, Kovacs AF, Kramer-Albers EM, Krasemann S,
624 Krause M, Kurochkin IV, Kusuma GD, Kuypers S, Laitinen S, Langevin SM, Languino LR, Lannigan J, Lasser
625 C, Laurent LC, Lavieu G, Lazaro-Ibanez E, Le Lay S, Lee MS, Lee YXF, Lemos DS, Lenassi M, Leszczynska
626 A, Li IT, Liao K, Libregts SF, Ligeti E, Lim R, Lim SK, Line A, Linnemannstons K, Llorente A, Lombard
627 CA, Lorenowicz MJ, Lorincz AM, Lotvall J, Lovett J, Lowry MC, Loyer X, Lu Q, Lukomska B, Lunavat TR,
628 Maas SL, Malhi H, Marcilla A, Mariani J, Mariscal J, Martens-Uzunova ES, Martin-Jaular L, Martinez MC,
629 Martins VR, Mathieu M, Mathivanan S, Maugeri M, McGinnis LK, McVey MJ, Meckes DG, Jr., Meehan KL,
630 Mertens I, Minciacci VR, Moller A, Moller Jorgensen M, Morales-Kastresana A, Morhayim J, Mullier F,
631 Muraca M, Musante L, Mussack V, Muth DC, Myburgh KH, Najrana T, Nawaz M, Nazarenko I, Nejsun P,
632 Neri C, Neri T, Nieuwland R, Nimrichter L, Nolan JP, Nolte-'t Hoen EN, Noren Hooten N, O'Driscoll L,
633 O'Grady T, O'Loghlen A, Ochiya T, Olivier M, Ortiz A, Ortiz LA, Osteikoetxea X, Ostergaard O, Ostrowski
634 M, Park J, Pegtel DM, Peinado H, Perut F, Pfaffl MW, Phinney DG, Pieters BC, Pink RC, Pisetsky DS, Pogge
635 von Strandmann E, Polakovicova I, Poon IK, Powell BH, Prada I, Pulliam L, Quesenberry P, Radeghieri A,
636 Raffai RL, Raimondo S, Rak J, Ramirez MI, Raposo G, Rayyan MS, Regev-Rudzki N, Ricklefs FL, Robbins
637 PD, Roberts DD, Rodrigues SC, Rohde E, Rome S, Rouschop KM, Rughetti A, Russell AE, Saa P, Sahoo S,
638 Salas-Huenuleo E, Sanchez C, Saugstad JA, Saul MJ, Schiffelers RM, Schneider R, Schoyen TH, Scott A,
639 Shahaj E, Sharma S, Shatnyeva O, Shekari F, Shelke GV, Shetty AK, Shiba K, Siljander PR, Silva AM,
640 Skowronek A, Snyder OL, 2nd, Soares RP, Sodar BW, Soekmadji C, Sotillo J, Stahl PD, Stoorvogel W, Stott
641 SL, Strasser EF, Swift S, Tahara H, Tewari M, Timms K, Tiwari S, Tixeira R, Tkach M, Toh WS, Tomasini
642 R, Torrecilhas AC, Tosar JP, Toxavidis V, Urbanelli L, Vader P, van Balkom BW, van der Grein SG, Van
643 Deun J, van Herwijnen MJ, Van Keuren-Jensen K, van Niel G, van Royen ME, van Wijnen AJ, Vasconcelos
644 MH, Vechetti IJ, Jr., Veit TD, Vella LJ, Velot E, Verweij FJ, Vestad B, Vinas JL, Visnovitz T, Vukman KV,
645 Wahlgren J, Watson DC, Wauben MH, Weaver A, Webber JP, Weber V, Wehman AM, Weiss DJ, Welsh JA,
646 Wendt S, Wheelock AM, Wiener Z, Witte L, Wolfram J, Xagorari A, Xander P, Xu J, Yan X, Yanez-Mo M,
647 Yin H, Yuana Y, Zappulli V, Zarubova J, Zekas V, Zhang JY, Zhao Z, Zheng L, Zheutlin AR, Zickler AM,
648 Zimmermann P, Zivkovic AM, Zocco D, Zuba-Surma EK: Minimal information for studies of extracellular
649 vesicles 2018 (MISEV2018): a position statement of the International Society for Extracellular Vesicles and
650 update of the MISEV2014 guidelines. *J Extracell Vesicles* 2018;7:1535750
- 651 15. Prattichizzo F, Giuliani A, Sabbatinelli J, Mensa E, De Nigris V, La Sala L, de Candia P, Olivieri F,
652 Ceriello A: Extracellular vesicles circulating in young organisms promote healthy longevity. *J Extracell*
653 *Vesicles* 2019;8:1656044
- 654 16. Prattichizzo F, Micolucci L, Cricca M, De Carolis S, Mensa E, Ceriello A, Procopio AD, Bonafe M,
655 Olivieri F: Exosome-based immunomodulation during aging: A nano-perspective on inflamm-aging. *Mech*
656 *Ageing Dev* 2017;168:44-53
- 657 17. Xiao Y, Zheng L, Zou X, Wang J, Zhong J, Zhong T: Extracellular vesicles in type 2 diabetes mellitus:
658 key roles in pathogenesis, complications, and therapy. *J Extracell Vesicles* 2019;8:1625677
- 659 18. Jansen F, Yang X, Hoelscher M, Cattelan A, Schmitz T, Proebsting S, Wenzel D, Vosen S, Franklin BS,
660 Fleischmann BK, Nickenig G, Werner N: Endothelial microparticle-mediated transfer of MicroRNA-126
661 promotes vascular endothelial cell repair via SPRED1 and is abrogated in glucose-damaged endothelial
662 microparticles. *Circulation* 2013;128:2026-2038
- 663 19. Sun Y, Shi H, Yin S, Ji C, Zhang X, Zhang B, Wu P, Shi Y, Mao F, Yan Y, Xu W, Qian H: Human
664 Mesenchymal Stem Cell Derived Exosomes Alleviate Type 2 Diabetes Mellitus by Reversing Peripheral
665 Insulin Resistance and Relieving beta-Cell Destruction. *ACS Nano* 2018;12:7613-7628

- 666 20. Castano C, Novials A, Parrizas M: Exosomes and diabetes. *Diabetes Metab Res Rev* 2019;35:e3107
- 667 21. Katayama M, Wiklander OPB, Fritz T, Caidahl K, El-Andaloussi S, Zierath JR, Krook A: Circulating
668 Exosomal miR-20b-5p Is Elevated in Type 2 Diabetes and Could Impair Insulin Action in Human Skeletal
669 Muscle. *Diabetes* 2019;68:515-526
- 670 22. Ghai V, Kim TK, Etheridge A, Nielsen T, Hansen T, Pedersen O, Galas D, Wang K: Extracellular Vesicle
671 Encapsulated MicroRNAs in Patients with Type 2 Diabetes Are Affected by Metformin Treatment. *J Clin Med*
672 2019;8
- 673 23. Florijn BW, Duijs J, Levels JH, Dallinga-Thie GM, Wang Y, Boing AN, Yuana Y, Stam W, Limpens R,
674 Au YW, Nieuwland R, Rabelink TJ, Reinders MEJ, van Zonneveld AJ, Bijkerk R: Diabetic Nephropathy
675 Alters the Distribution of Circulating Angiogenic MicroRNAs Among Extracellular Vesicles, HDL, and Ago-
676 2. *Diabetes* 2019;68:2287-2300
- 677 24. Thomou T, Mori MA, Dreyfuss JM, Konishi M, Sakaguchi M, Wolfrum C, Rao TN, Winnay JN, Garcia-
678 Martin R, Grinspoon SK, Gorden P, Kahn CR: Adipose-derived circulating miRNAs regulate gene expression
679 in other tissues. *Nature* 2017;542:450-455
- 680 25. Prattichizzo F, De Nigris V, Spiga R, Mancuso E, La Sala L, Antonicelli R, Testa R, Procopio AD, Olivieri
681 F, Ceriello A: Inflammageing and metaflammation: The yin and yang of type 2 diabetes. *Ageing Res Rev*
682 2018;41:1-17
- 683 26. Kaur R, Kaur M, Singh J: Endothelial dysfunction and platelet hyperactivity in type 2 diabetes mellitus:
684 molecular insights and therapeutic strategies. *Cardiovasc Diabetol* 2018;17:121
- 685 27. Clayton A, Court J, Navabi H, Adams M, Mason MD, Hobot JA, Newman GR, Jasani B: Analysis of
686 antigen presenting cell derived exosomes, based on immuno-magnetic isolation and flow cytometry. *J*
687 *Immunol Methods* 2001;247:163-174
- 688 28. Testa R, Olivieri F, Sirolla C, Spazzafumo L, Rippo MR, Marra M, Bonfigli AR, Ceriello A, Antonicelli
689 R, Franceschi C, Castellucci C, Testa I, Procopio AD: Leukocyte telomere length is associated with
690 complications of type 2 diabetes mellitus. *Diabet Med* 2011;28:1388-1394
- 691 29. American Diabetes A: 2. Classification and Diagnosis of Diabetes: Standards of Medical Care in Diabetes-
692 2019. *Diabetes Care* 2019;42:S13-S28
- 693 30. Testa R, Bonfigli AR, Salvioli S, Invidia L, Pierini M, Sirolla C, Marra M, Testa I, Fazioli F, Recchioni
694 R, Marcheselli F, Olivieri F, Lanari L, Franceschi C: The Pro/Pro genotype of the p53 codon 72 polymorphism
695 modulates PAI-1 plasma levels in ageing. *Mech Ageing Dev* 2009;130:497-500
- 696 31. Olivieri F, Bonafe M, Spazzafumo L, Gobbi M, Prattichizzo F, Recchioni R, Marcheselli F, La Sala L,
697 Galeazzi R, Rippo MR, Fulgenzi G, Angelini S, Lazzarini R, Bonfigli AR, Bruge F, Tiano L, Genovese S,
698 Ceriello A, Boemi M, Franceschi C, Procopio AD, Testa R: Age- and glycemia-related miR-126-3p levels in
699 plasma and endothelial cells. *Aging (Albany NY)* 2014;6:771-787
- 700 32. Mensa E, Giuliani A, Matakchione G, Gurau F, Bonfigli AR, Romagnoli F, De Luca M, Sabbatinelli J,
701 Olivieri F: Circulating miR-146a in healthy aging and type 2 diabetes: Age- and gender-specific trajectories.
702 *Mech Ageing Dev* 2019;180:1-10
- 703 33. Consortium E-T, Van Deun J, Mestdagh P, Agostinis P, Akay O, Anand S, Anckaert J, Martinez ZA,
704 Baetens T, Beghein E, Bertier L, Berx G, Boere J, Boukouris S, Bremer M, Buschmann D, Byrd JB, Casert C,
705 Cheng L, Cmoch A, Daveloose D, De Smedt E, Demirsoy S, Depoorter V, Dhondt B, Driedonks TA, Dudek
706 A, Elsharawy A, Floris I, Foers AD, Gartner K, Garg AD, Geurickx E, Gettemans J, Ghazavi F, Giebel B,
707 Kormelink TG, Hancock G, Helmoortel H, Hill AF, Hyenne V, Kalra H, Kim D, Kowal J, Kraemer S,
708 Leidinger P, Leonelli C, Liang Y, Lippens L, Liu S, Lo Cicero A, Martin S, Mathivanan S, Mathiyalagan P,
709 Matusek T, Milani G, Monguio-Tortajada M, Mus LM, Muth DC, Nemeth A, Nolte-t Hoen EN, O'Driscoll L,
710 Palmulli R, Pfaffl MW, Primdal-Bengtson B, Romano E, Rousseau Q, Sahoo S, Sampaio N, Samuel M,

- 711 Scicluna B, Soen B, Steels A, Swinnen JV, Takatalo M, Thaminy S, Thery C, Tulkens J, Van Audenhove I,
712 van der Grein S, Van Goethem A, van Herwijnen MJ, Van Niel G, Van Roy N, Van Vliet AR, Vandamme N,
713 Vanhauwaert S, Vergauwen G, Verweij F, Wallaert A, Wauben M, Witwer KW, Zonneveld MI, De Wever O,
714 Vandesompele J, Hendrix A: EV-TRACK: transparent reporting and centralizing knowledge in extracellular
715 vesicle research. *Nat Methods* 2017;14:228-232
- 716 34. Gardiner C, Ferreira YJ, Dragovic RA, Redman CW, Sargent IL: Extracellular vesicle sizing and
717 enumeration by nanoparticle tracking analysis. *J Extracell Vesicles* 2013;2
- 718 35. Koliha N, Wiencek Y, Heider U, Jungst C, Kladt N, Krauthauser S, Johnston IC, Bosio A, Schauss A,
719 Wild S: A novel multiplex bead-based platform highlights the diversity of extracellular vesicles. *J Extracell*
720 *Vesicles* 2016;5:29975
- 721 36. Metsalu T, Vilo J: ClustVis: a web tool for visualizing clustering of multivariate data using Principal
722 Component Analysis and heatmap. *Nucleic Acids Res* 2015;43:W566-570
- 723 37. Heberle H, Meirelles GV, da Silva FR, Telles GP, Minghim R: InteractiVenn: a web-based tool for the
724 analysis of sets through Venn diagrams. *BMC Bioinformatics* 2015;16:169
- 725 38. Mensà E, Guescini M, Giuliani A, Bacalini MG, Ramini D, Corleone G, Ferracin M, Fulgenzi G, Graciotti
726 L, Prattichizzo F, Sorci L, Battistelli M, Monsurrò V, Bonfigli AR, Cardelli M, Recchioni R, Marcheselli F,
727 Latini S, Maggio S, Fanelli M, Amatori S, Storci G, Ceriello A, Stocchi V, De Luca M, Magnani L, Rippo
728 MR, Procopio AD, Sala C, Budimir I, Bassi C, Negrini M, Garagnani P, Franceschi C, Sabbatinelli J, Bonafè
729 M, Olivieri F: Small extracellular vesicles deliver miR-21 and miR-217 as pro-senescence effectors to
730 endothelial cells. *Journal of Extracellular Vesicles* 2020;9:1725285
- 731 39. Prattichizzo F, De Nigris V, Mancuso E, Spiga R, Giuliani A, Maticchione G, Lazzarini R, Marcheselli F,
732 Recchioni R, Testa R, La Sala L, Rippo MR, Procopio AD, Olivieri F, Ceriello A: Short-term sustained
733 hyperglycaemia fosters an archetypal senescence-associated secretory phenotype in endothelial cells and
734 macrophages. *Redox Biol* 2018;15:170-181
- 735 40. Keller A, Fehlmann T, Ludwig N, Kahraman M, Laufer T, Backes C, Vogelmeier C, Diener C, Biertz F,
736 Herr C, Jorres RA, Lenhof HP, Meese E, Bals R, Group CS: Genome-wide MicroRNA Expression Profiles in
737 COPD: Early Predictors for Cancer Development. *Genomics Proteomics Bioinformatics* 2018;16:162-171
- 738 41. DeLong ER, DeLong DM, Clarke-Pearson DL: Comparing the areas under two or more correlated receiver
739 operating characteristic curves: a nonparametric approach. *Biometrics* 1988;44:837-845
- 740 42. Turchinovich A, Samatov TR, Tonevitsky AG, Burwinkel B: Circulating miRNAs: cell-cell
741 communication function? *Front Genet* 2013;4:119
- 742 43. Turchinovich A, Weiz L, Langhein A, Burwinkel B: Characterization of extracellular circulating
743 microRNA. *Nucleic Acids Res* 2011;39:7223-7233
- 744 44. Kaudewitz D, Skroblin P, Bender LH, Barwari T, Willeit P, Pechlaner R, Sunderland NP, Willeit K,
745 Morton AC, Armstrong PC, Chan MV, Lu R, Yin X, Gracio F, Dudek K, Langley SR, Zampetaki A, de
746 Rinaldis E, Ye S, Warner TD, Saxena A, Kiechl S, Storey RF, Mayr M: Association of MicroRNAs and
747 YRNAs With Platelet Function. *Circ Res* 2016;118:420-432
- 748 45. van Balkom BW, Eisele AS, Pegtel DM, Bervoets S, Verhaar MC: Quantitative and qualitative analysis of
749 small RNAs in human endothelial cells and exosomes provides insights into localized RNA processing,
750 degradation and sorting. *J Extracell Vesicles* 2015;4:26760
- 751 46. Sharma H, Chinnappan M, Agarwal S, Dalvi P, Gunewardena S, O'Brien-Ladner A, Dhillon NK:
752 Macrophage-derived extracellular vesicles mediate smooth muscle hyperplasia: role of altered miRNA cargo
753 in response to HIV infection and substance abuse. *FASEB J* 2018;32:5174-5185

- 754 47. Willeit P, Zampetaki A, Dudek K, Kaudewitz D, King A, Kirkby NS, Crosby-Nwaobi R, Prokopi M,
755 Drozdov I, Langley SR, Sivaprasad S, Markus HS, Mitchell JA, Warner TD, Kiechl S, Mayr M: Circulating
756 microRNAs as novel biomarkers for platelet activation. *Circ Res* 2013;112:595-600
- 757 48. Barwari T, Joshi A, Mayr M: MicroRNAs in Cardiovascular Disease. *J Am Coll Cardiol* 2016;68:2577-
758 2584
- 759 49. Willeit P, Skrobilin P, Kiechl S, Fernandez-Hernando C, Mayr M: Liver microRNAs: potential mediators
760 and biomarkers for metabolic and cardiovascular disease? *Eur Heart J* 2016;37:3260-3266
- 761 50. Jansen F, Wang H, Przybilla D, Franklin BS, Dolf A, Pfeifer P, Schmitz T, Flender A, Endl E, Nickenig
762 G, Werner N: Vascular endothelial microparticles-incorporated microRNAs are altered in patients with
763 diabetes mellitus. *Cardiovasc Diabetol* 2016;15:49
- 764 51. Jansen F, Li Q, Pfeifer A, Werner N: Endothelial- and Immune Cell-Derived Extracellular Vesicles in the
765 Regulation of Cardiovascular Health and Disease. *JACC Basic Transl Sci* 2017;2:790-807
- 766 52. Zampetaki A, Willeit P, Tilling L, Drozdov I, Prokopi M, Renard JM, Mayr A, Weger S, Schett G, Shah
767 A, Boulanger CM, Willeit J, Chowienczyk PJ, Kiechl S, Mayr M: Prospective study on circulating MicroRNAs
768 and risk of myocardial infarction. *J Am Coll Cardiol* 2012;60:290-299
- 769 53. Freeman DW, Noren Hooten N, Eitan E, Green J, Mode NA, Bodogai M, Zhang Y, Lehrmann E,
770 Zonderman AB, Biragyn A, Egan J, Becker KG, Mattson MP, Ejiogu N, Evans MK: Altered Extracellular
771 Vesicle Concentration, Cargo, and Function in Diabetes. *Diabetes* 2018;67:2377-2388
- 772 54. Boulton AJ, Vinik AI, Arezzo JC, Bril V, Feldman EL, Freeman R, Malik RA, Maser RE, Sosenko JM,
773 Ziegler D, American Diabetes A: Diabetic neuropathies: a statement by the American Diabetes Association.
774 *Diabetes Care* 2005;28:956-962
- 775 55. Salomon C, Scholz-Romero K, Sarker S, Sweeney E, Kobayashi M, Correa P, Longo S, Duncombe G,
776 Mitchell MD, Rice GE, Illanes SE: Gestational Diabetes Mellitus Is Associated With Changes in the
777 Concentration and Bioactivity of Placenta-Derived Exosomes in Maternal Circulation Across Gestation.
778 *Diabetes* 2016;65:598-609
- 779 56. Prattichizzo F, Giuliani A, Sabbatinelli J, Matakchione G, Ramini D, Bonfigli AR, Rippo MR, de Candia
780 P, Procopio AD, Olivieri F, Ceriello A: Prevalence of residual inflammatory risk and associated clinical
781 variables in patients with type 2 diabetes. *Diabetes Obes Metab* 2020;
- 782 57. Togliatto G, Dentelli P, Rosso A, Lombardo G, Gili M, Gallo S, Gai C, Solini A, Camussi G, Brizzi MF:
783 PDGF-BB Carried by Endothelial Cell-Derived Extracellular Vesicles Reduces Vascular Smooth Muscle Cell
784 Apoptosis in Diabetes. *Diabetes* 2018;67:704-716
- 785 58. Xiong Y, Chen L, Yan C, Zhou W, Endo Y, Liu J, Hu L, Hu Y, Mi B, Liu G: Circulating Exosomal miR-
786 20b-5p Inhibition Restores Wnt9b Signaling and Reverses Diabetes-Associated Impaired Wound Healing.
787 *Small* 2019:e1904044
- 788 59. Zampetaki A, Kiechl S, Drozdov I, Willeit P, Mayr U, Prokopi M, Mayr A, Weger S, Oberhollenzer F,
789 Bonora E, Shah A, Willeit J, Mayr M: Plasma microRNA profiling reveals loss of endothelial miR-126 and
790 other microRNAs in type 2 diabetes. *Circ Res* 2010;107:810-817
- 791 60. Fejes Z, Poliska S, Czimmerer Z, Kaplar M, Penyige A, Gal Szabo G, Beke Debreceni I, Kunapuli SP,
792 Kappelmayer J, Nagy B, Jr.: Hyperglycaemia suppresses microRNA expression in platelets to increase
793 P2RY12 and SELP levels in type 2 diabetes mellitus. *Thromb Haemost* 2017;117:529-542
- 794 61. Ryu HS, Park SY, Ma D, Zhang J, Lee W: The induction of microRNA targeting IRS-1 is involved in the
795 development of insulin resistance under conditions of mitochondrial dysfunction in hepatocytes. *PLoS One*
796 2011;6:e17343

- 797 62. Fernandez-Twinn DS, Alfaradhi MZ, Martin-Gronert MS, Duque-Guimaraes DE, Piekarz A, Ferland-
798 McCollough D, Bushell M, Ozanne SE: Downregulation of IRS-1 in adipose tissue of offspring of obese mice
799 is programmed cell-autonomously through post-transcriptional mechanisms. *Mol Metab* 2014;3:325-333
- 800 63. Zang J, Maxwell AP, Simpson DA, McKay GJ: Differential Expression of Urinary Exosomal MicroRNAs
801 miR-21-5p and miR-30b-5p in Individuals with Diabetic Kidney Disease. *Sci Rep* 2019;9:10900
802
- 803 64. Simonsen JB: Pitfalls associated with lipophilic fluorophore staining of extracellular vesicles for uptake
804 studies. *J Extracell Vesicles*. 2019 Feb 20;8(1):1582237.
805
- 806 65. Witwer KW, Buzás EI, Bemis LT, Bora A, Lässer C, Lötvall J, Nolte-t Hoen EN, Piper MG, Sivaraman
807 S, Skog J, Théry C, Wauben MH, Hochberg F: Standardization of sample collection, isolation and analysis
808 methods in extracellular vesicle research. *J Extracell Vesicles*. 2013 May 27;2.
809

810 **TABLES**811 **Table 1.** Demographic, clinical, and biochemical characteristics of the 218 enrolled subjects.

812 Variables are expressed as mean (standard deviation). P value from ANOVA for continuous variables

813 and from chi squared tests of association for categorical variables. *, p<0.05 vs. CTR; #, p<0.05 vs.

814 T2DM-NC.

815

| Variables | CTR (N=60) | T2DM-NC (N=57) | T2DM-C (N=101) | p-value |
|--------------------------------|----------------|-------------------|-------------------|---------|
| Age (years) | 66.4 (9.9) | 64.4 (9.3) | 67.5 (8.0) | 0.112 |
| Gender (males) | 35 | 32 | 71 | 0.134 |
| BMI (Kg/m ²) | 26.0 (4.1) | 29.0 (5.1) * | 28.5 (4.4) * | <0.001 |
| Waist-hip ratio | 0.86 (0.08) | 0.93 (0.07) * | 0.95 (0.065) * | <0.001 |
| Total cholesterol (mg/dL) | 220.6 (41.4) | 216.2 (40.1) | 197.1 (40.1) *# | 0.001 |
| LDL-C (mg/dL) | 126.5 (34.8) | 129.0 (34.7) | 107.9 (30.8) *# | <0.001 |
| HDL-C (mg/dL) | 62.8 (16.2) | 51.9 (16.0) * | 49.5 (12.8) * | <0.001 |
| Triglycerides (mg/dL) | 107.98 (82.29) | 162.39 (123.90) * | 139.65 (95.05) | 0.014 |
| Glucose (mg/dL) | 95.58 (10.021) | 154.72 (50.292) * | 176.64 (51.768) * | <0.001 |
| HbA1C (%) | 5.913 (0.396) | 7.358 (1.149) * | 7.768 (1.281) * | <0.001 |
| Insulin (UI/mL) | 5.108 (2.941) | 10.704 (18.396) * | 6.273 (4.789) # | 0.006 |
| HOMA index | 1.22 (0.71) | 4.43 (7.24) * | 2.77 (2.32) *# | <0.001 |
| WBC (n/mm ³) | 5.99 (1.36) | 6.55 (1.81) | 6.70 (1.58) * | 0.023 |
| Platelets (n/mm ³) | 225.1 (50.0) | 222.2 (54.0) | 214.1 (62.0) | 0.447 |
| hs-CRP (mg/L) | 2.25 (2.48) | 2.70 (2.26) | 2.58 (8.81) | 0.539 |
| Creatinine (mg/dL) | 0.81 (0.17) | 0.84 (0.22) | 1.04 (0.39) *# | <0.001 |
| Azotemia (mg/dL) | 37.3 (8.7) | 37.7 (11.5) | 44.0 (18.5) *# | 0.006 |
| eGFR (mL/min) | 83.2 (16.1) | 82.9 (22.6) | 72.3 (20.7) *# | 0.001 |
| Uric acid (mg/dL) | 4.60 (1.26) | 4.95 (1.46) | 4.85 (1.19) | 0.305 |

816

817

818

819

820

821

822 **Table 2.** Binary logistic regression analyses of miRNAs associated with major adverse cardiovascular
 823 events (MACE) in T2DM patients (a), and evaluation of the predictive value for MACE of the 4-
 824 miRNA model (see Table 3) (b) and of the 4-miRNA model after global-mean normalization (c)
 825 when adjusted for the conventional risk factors. Where applicable, odds ratio (95% CI) are expressed
 826 per 0.5 SD increase of each miRNA.

827

| a) 4-miRNA model + risk factors (enter method) | | | | |
|---|----------|-----------|----------------|--|
| Variable | B | SE | P value | |
| 4-miRNA signature | 9.601 | 1.753 | <0.001 | |
| Age | 0.072 | 0.040 | 0.073 | |
| Gender (reference category: female) | 0.828 | 0.625 | 0.185 | |
| Hypertension | 0.042 | 0.683 | 0.951 | |
| HbA1c | 0.354 | 0.216 | 0.100 | |
| LDL | 0.001 | 0.008 | 0.878 | |
| b) 4-miRNA model (global mean normalization) + risk factors (enter method) | | | | |
| Variable | B | SE | P value | |
| 4-miRNA signature | 7.267 | 1.270 | <0.001 | |
| Age | 0.060 | 0.035 | 0.082 | |
| Gender (reference category: female) | 1.135 | 0.563 | 0.044 | |
| Hypertension | -0.358 | 0.597 | 0.549 | |
| HbA1c | 0.435 | 0.202 | 0.031 | |
| LDL | -0.003 | 0.008 | 0.665 | |
| c) 11-miRNA model (backward method) | | | | |
| miRNA | B | SE | P value | OR (95% CI) |
| miR-155 | -12.749 | 5.202 | 0.014 | 3×10 ⁻⁶ (1.084×10 ⁻¹⁰ – 0.078) |
| miR-195-5p | 3.032 | 1.999 | 0.129 | 20.737 (0.412 – 1043.745) |
| miR-24-3p | -4.039 | 3.641 | 0.267 | 0.018 (1.4×10 ⁻⁵ – 22.126) |
| miR-320a | 0.997 | 0.410 | 0.015 | 2.709 (1.213 – 6.054) |
| miR-342-3p | 0.704 | 0.304 | 0.021 | 2.021 (1.113 – 3.670) |
| miR-376a | 0.898 | 0.371 | 0.015 | 2.454 (1.186 – 5.076) |
| miR-451a | -1.010 | 0.354 | 0.004 | 0.364 (0.182 – 0.728) |

828

829

830 **FIGURE LEGENDS**

831 **Figure 1. Isolation and characterization of CD31⁺ extracellular vesicles.** (A) Schematic
832 representation of the isolation method. (B) Nanoparticle tracking analysis (NTA) of one
833 representative sample of isolated CD31⁺ EVs, along with the observed mean size and number (from
834 1 ml of pooled control plasma). (C) Representative TEM image of EVs isolated with CD31 beads
835 along with the relative magnification. (D) Western blot showing the expression of CD31, Alix,
836 TSG101, CD63, ApoB100 and ApoA1 in CD31⁺ EVs and ultracentrifugation (UC)-collected EVs
837 isolated from the same amount of plasma, along with the relative densitometric analysis. Whole
838 plasma was run as positive control for ApoA1 and ApoB100. (E) Ratio between the expression of
839 CD31 and CD9, CD63, or CD81 in CD31⁺ EVs vs EVs isolated through UC, as measured with a
840 specific kit allowing cytofluorimetric detection (n=6 from pooled plasma split to perform
841 comparative isolation starting from the same volume). (F) Comparative cytofluorimetric detection of
842 CD49e, CD9, CD63, CD62P, CD81, CD41b, CD42a, CD29, and CD69 in EVs isolated with no beads,
843 scramble IgG beads, and CD31 beads (n=3, from equal amount of control plasma samples). (G)
844 Concentration of collected CD31⁺ EVs vs the CD31 depleted fraction of EVs subjected to UC,
845 measured with standard NTA (n=3); (H) RT-PCR dosage of miR-126-3p, miR-146a-5p, miR-155,
846 and miR-21-5p in whole plasma vs total EVs isolated with UC vs CD31⁺EVs, dividing the same
847 control samples in different aliquots (same volume, 100 μ l) to compare the relative abundance in the
848 various compartments (n=8). Errors bar are \pm SD. *p<0.05, **p<0.01 Student's *t* test for panels D,
849 E, and G; One-way ANOVA for panels F and H.

850

851 **Figure 2. Comparative concentration, modal size and miRNA profiling of CD31⁺ EVs from**
852 **controls and patients with T2DM.** NTA measurement of the concentration (A) and modal size (B)
853 of CD31⁺ EVs isolated from healthy controls and patients with T2DM (n=4); (C) Comparative
854 cytofluorimetric detection of CD31, CD9, CD63, and CD81 of CD31⁺ EVs isolated from controls

855 and patients with T2DM (n=4). (D) Heatmap showing miRNAs profiling in CD31⁺EVs from controls
856 and patients with T2DM (n=5 vs 5, pooled samples). *p<0.05, Student's t test

857

858 **Figure 3. Expression levels of 11 miRNAs in CD31⁺EVs from healthy controls, patients with**
859 **non-complicated T2DM (T2DM-NC) and patients with T2DM and complications (T2DM-C).**

860 Violin plots with individual points showing the expression of miR-126-3p, miR-146a-5p, miR-155,
861 miR-195-5p, miR-21-5p, miR-24-3p, miR-320a, miR-342-3p, miR-376a, miR-422, and miR-451a in
862 in a cohort of 218 individuals, 60 healthy (Ctrl), 57 with uncomplicated T2DM (T2DM-NC), and 101
863 with T2DM and complications (T2DM-C). **p<0.05, ***p<0.01 Kruskal-Wallis followed by Dunn
864 post hoc test.

865

866 **Figure 4. Diagnostic performance of the differentially expressed miRNAs in CD31⁺EVs.**

867 Receiving operator curves (ROC) and the relative area under the curve (AUC) for differentially
868 expressed miRNAs showing the diagnostic performance for T2DM vs Ctrl (A), T2DM-C vs T2DM-
869 NC (B). ROC curves for miR-146a-5p and miR-21-5p shuttled in CD31⁺ EVs compared with those
870 of the same miRNAs measured in the same amount of whole plasma with the relative diagnostic
871 performance to detect T2DM vs Ctrl (C) and T2DM-C vs T2DM-NC (D).

872

873 **Figure 5. Correlations between tested miRNAs and clinical variables and reciprocal among**

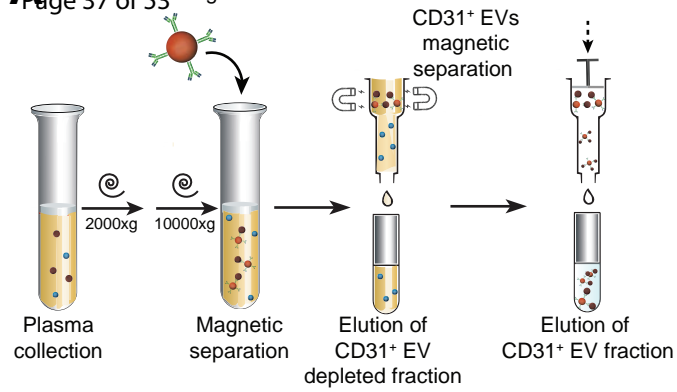
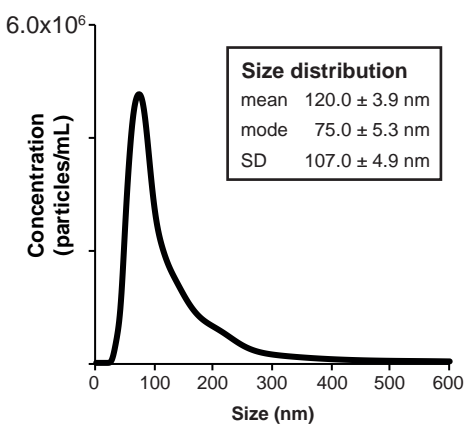
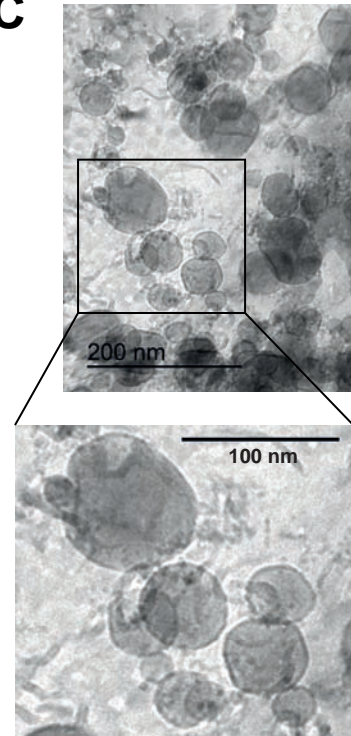
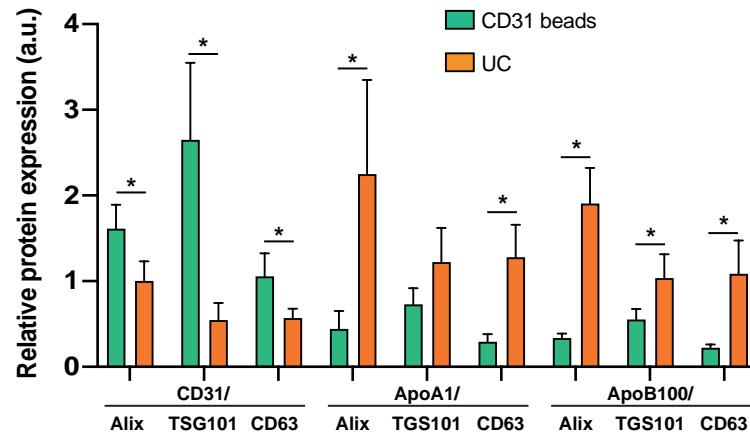
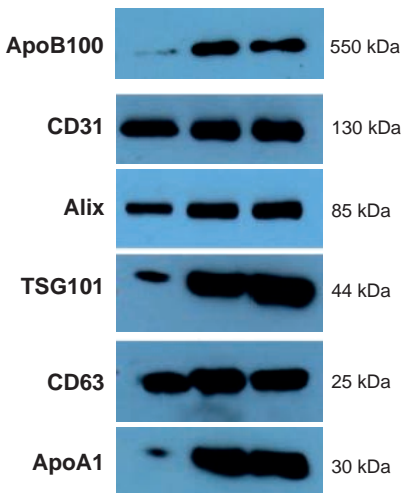
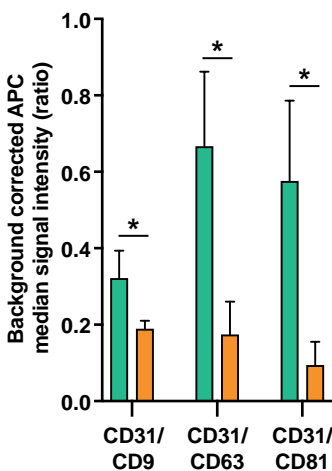
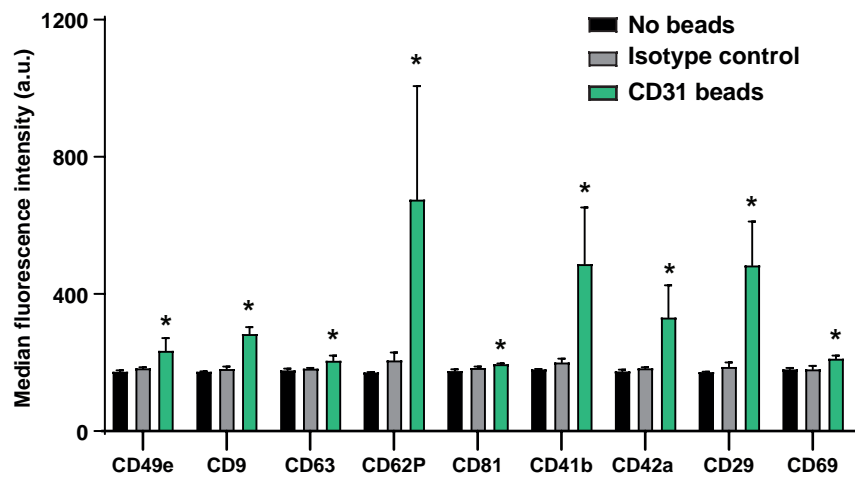
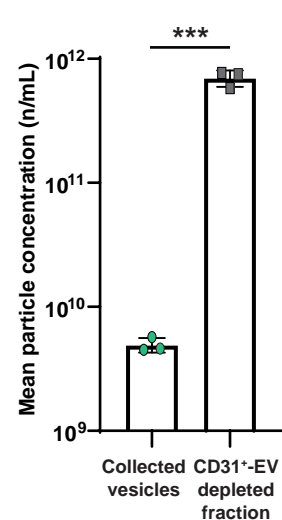
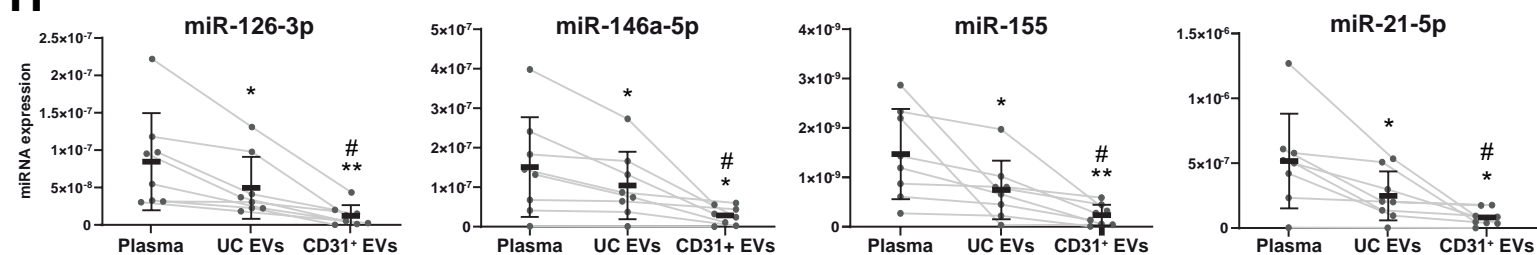
874 **miRNAs.** Color-coded correlogram showing the significant Pearson's correlations between tested
875 miRNAs and clinical variables (A) and the reciprocal correlations between miRNAs (B). The
876 intensity of the colour and the dimension of the points depend on the magnitude of the correlation.

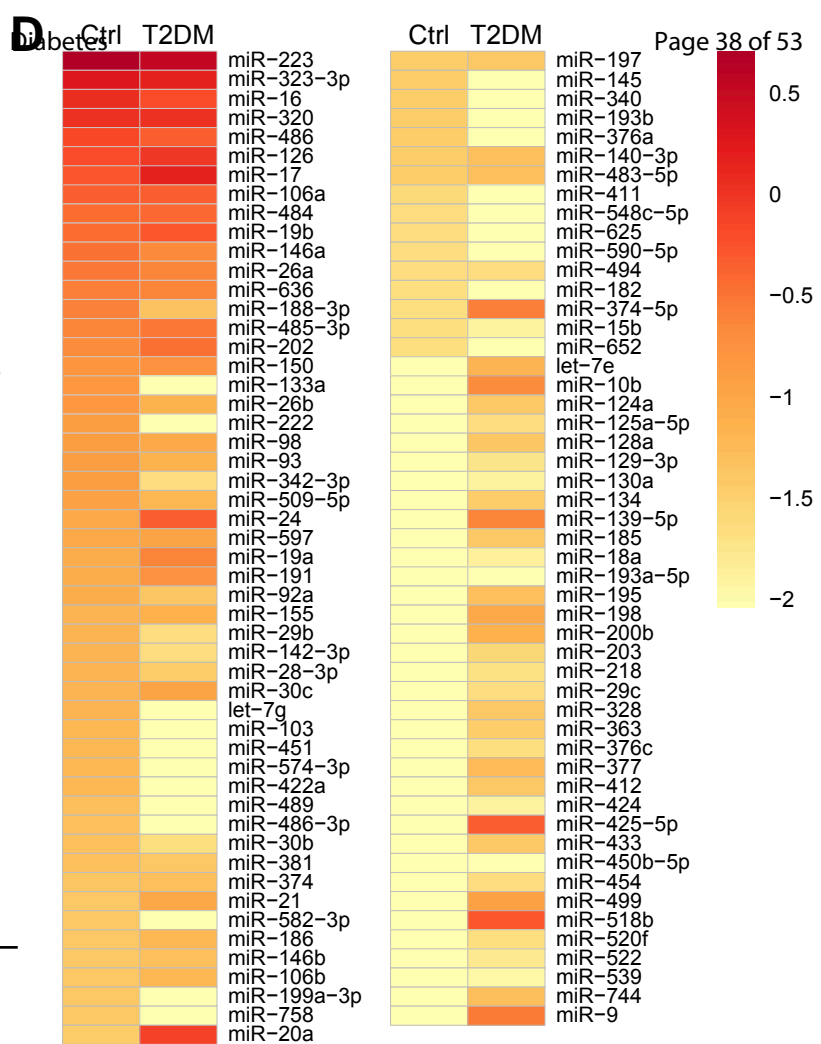
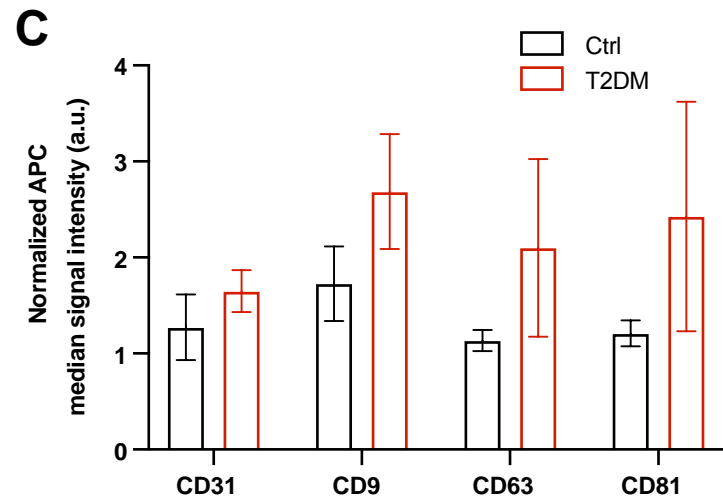
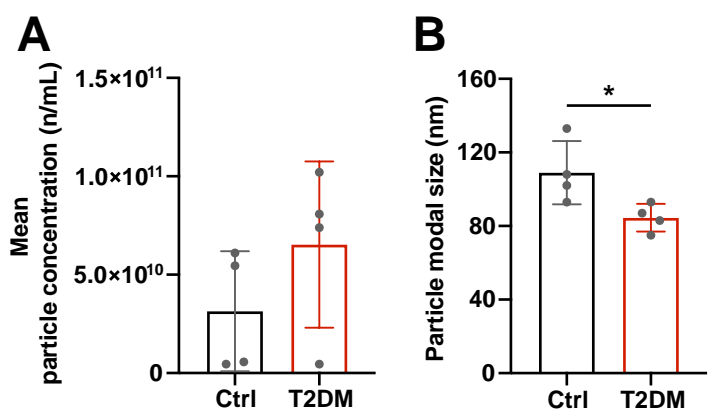
877

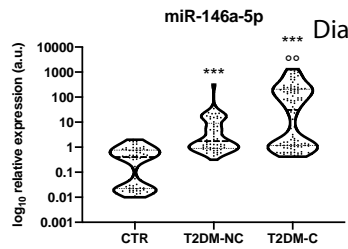
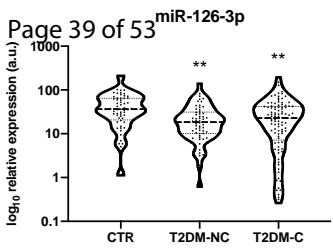
878 **Figure 6. *In vitro* treatment of endothelial cells with CD31⁺ EVs.** (A) Schematic representation

879 of the method used to detach EVs from beads; (B) Representative image of endothelial cells treated
880 for 24h with EVs previously stained with a fluorescent green, lipophilic dye (PKH67), and stained

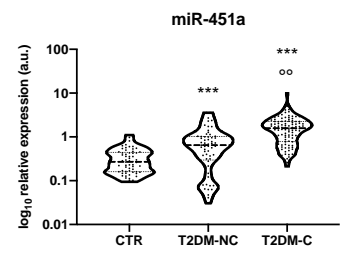
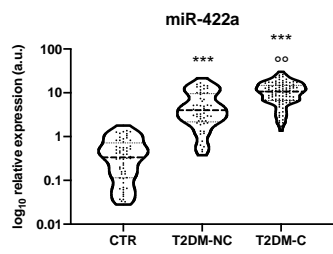
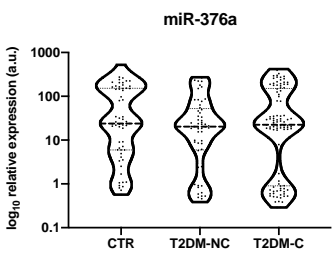
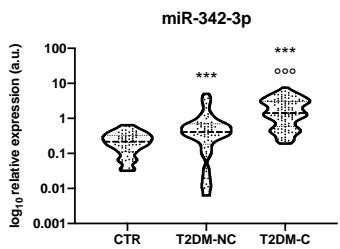
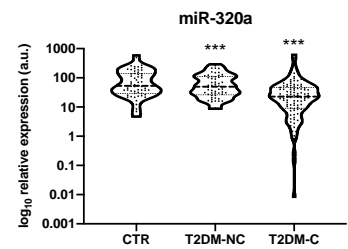
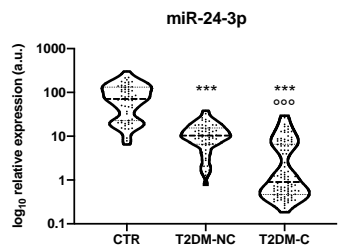
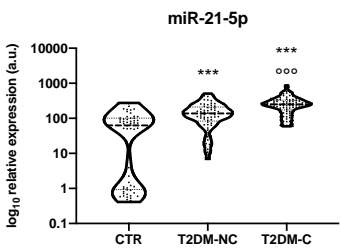
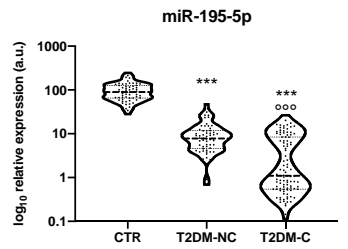
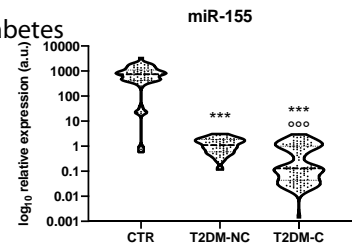
881 with DAPI to evidence cell nuclei. The relative merge is also shown. (C) Representative image of
882 endothelial cells treated for 24h with EVs previously loaded with a fluorescent (Texas Red), small
883 RNA and stained with DAPI. (D) Relative expression of the non-human *cel-miR-39* in endothelial
884 cells treated with EVs transfected with *cel-miR-39* or with the same of amount of the miRNA without
885 EVs (n=3) ***p<0.01 Student's t test. (E) mRNA expression of *CCL2*, *IL-1 α* , *TNF α* , *IL-6*, *CXCL-1*,
886 and *CXCL-8* in endothelial cells treated with EVs derived from controls, T2DM-NC, and T2DM-C
887 (n=3) *p<0.05, **p<0.01 One-way ANOVA.

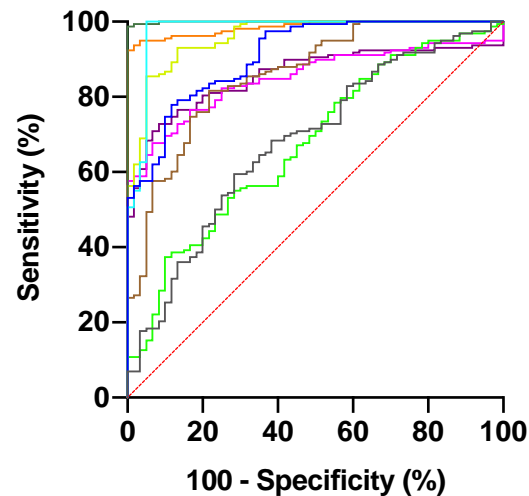
A Page 37 of 33 CD31 magnetic beads**B** Diabetes**C****D** CD31⁺ UC Plasma**E****F****G****H**



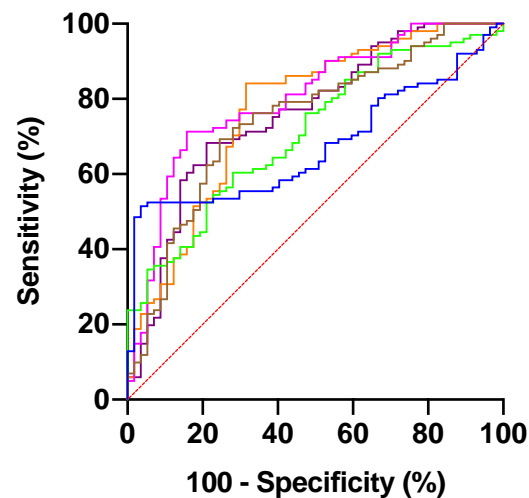


Diabetes



A**Ctrl vs. T2DM**

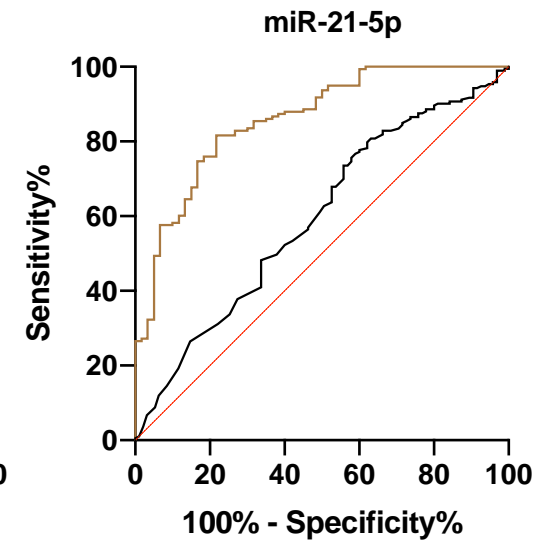
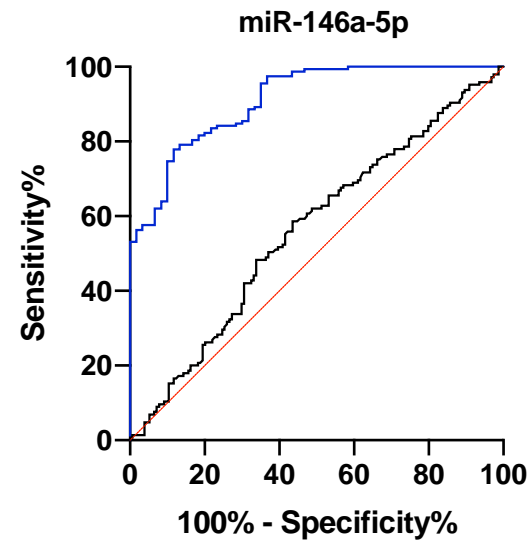
| miRNA | AUC | p value |
|-------------|-------|---------|
| miR-126-3p | 0.679 | <0.0001 |
| miR-146a-5p | 0.911 | <0.0001 |
| miR-155 | 0.978 | <0.0001 |
| miR-195-5p | 0.999 | <0.0001 |
| miR-21-5p | 0.859 | <0.0001 |
| miR-24-3p | 0.960 | <0.0001 |
| miR-320a | 0.673 | <0.0001 |
| miR-342-3p | 0.850 | <0.0001 |
| miR-422a | 0.985 | <0.0001 |
| miR-451a | 0.857 | <0.0001 |

B**T2DM-NC vs. T2DM-C**

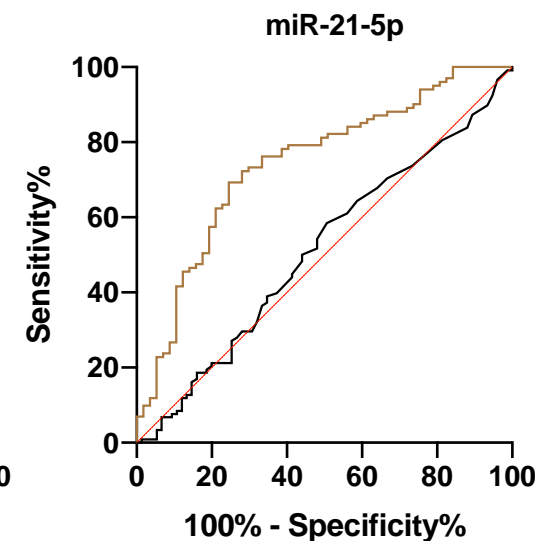
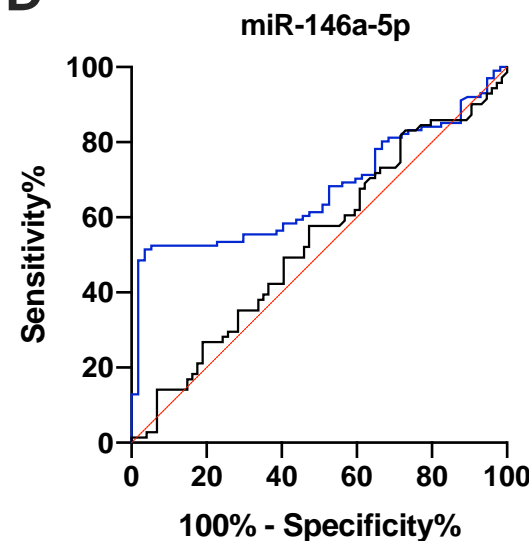
| miRNA | AUC | p value |
|-------------|-------|---------|
| miR-146a-5p | 0.673 | 0.0003 |
| miR-21-5p | 0.744 | <0.0001 |
| miR-320a | 0.709 | <0.0001 |
| miR-342-3p | 0.801 | <0.0001 |
| miR-422a | 0.770 | <0.0001 |
| miR-451a | 0.769 | <0.0001 |

C

Diabetes

Ctrl vs. T2DM

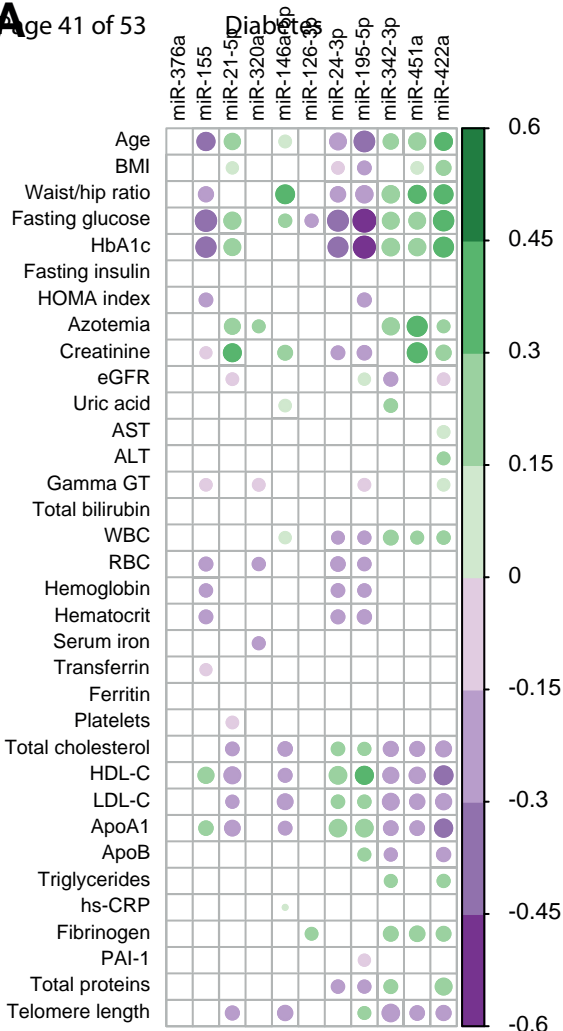
| miRNA | AUC | p value |
|-------------------------|-------|---------|
| miR-146a-5p | | |
| — Plasma | 0.562 | 0.064 |
| — CD31 ⁺ EVs | 0.911 | <0.0001 |
| miR-21-5p | | |
| — Plasma | 0.595 | 0.009 |
| — CD31 ⁺ EVs | 0.859 | <0.0001 |

D**T2DM-NC vs. T2DM-C**

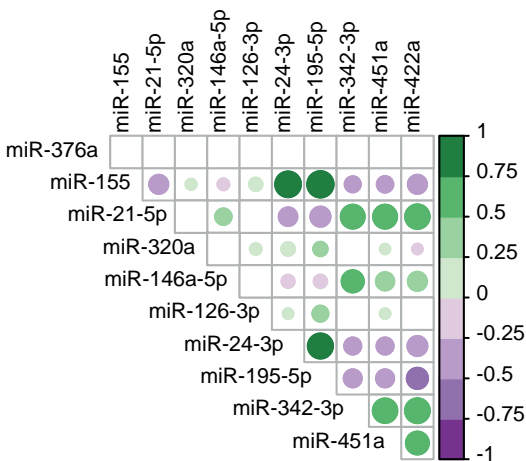
| miRNA | AUC | p value |
|-------------------------|-------|---------|
| miR-146a-5p | | |
| — Plasma | 0.533 | 0.496 |
| — CD31 ⁺ EVs | 0.673 | <0.001 |
| miR-21-5p | | |
| — Plasma | 0.511 | 0.798 |
| — CD31 ⁺ EVs | 0.744 | <0.0001 |

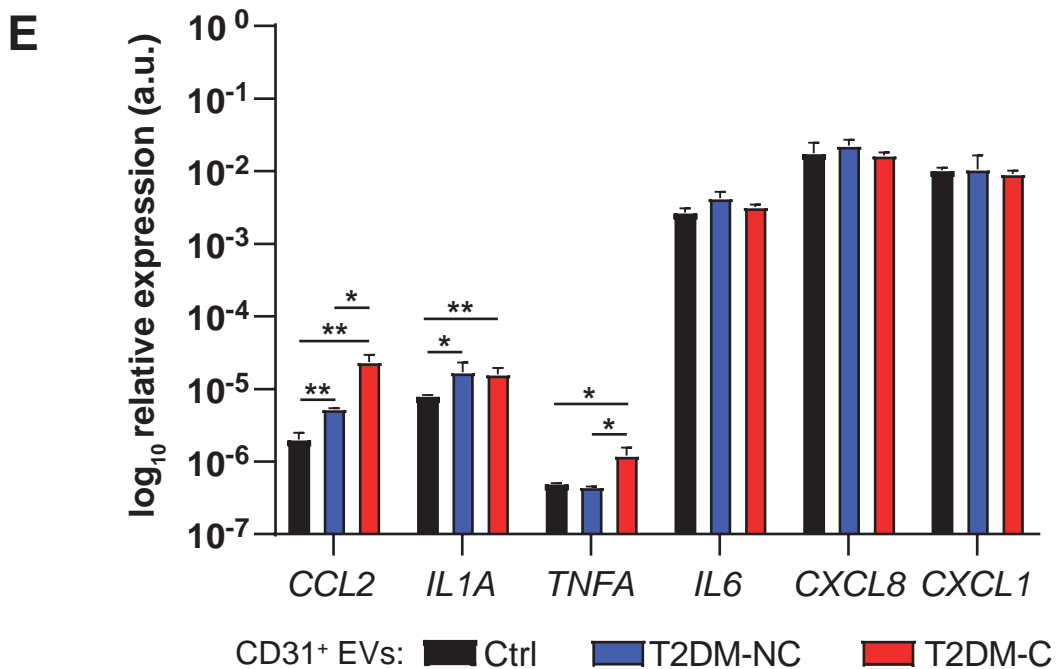
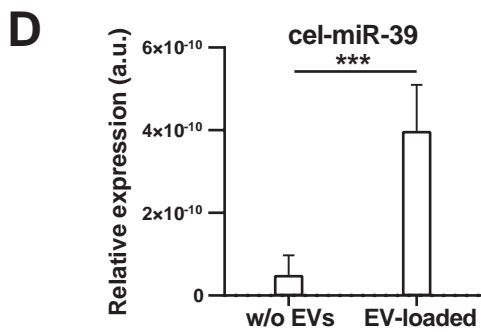
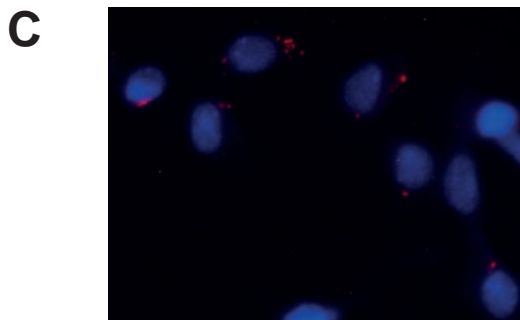
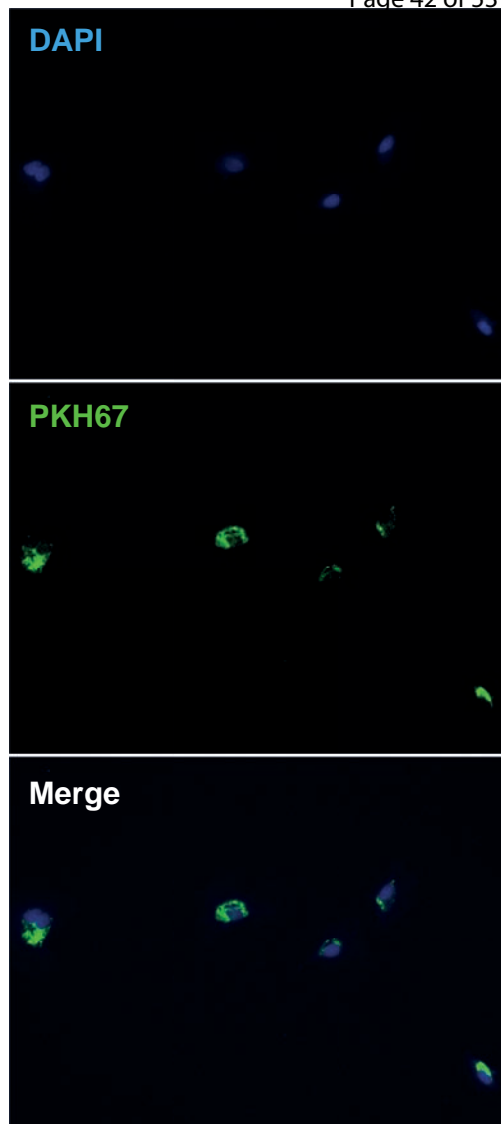
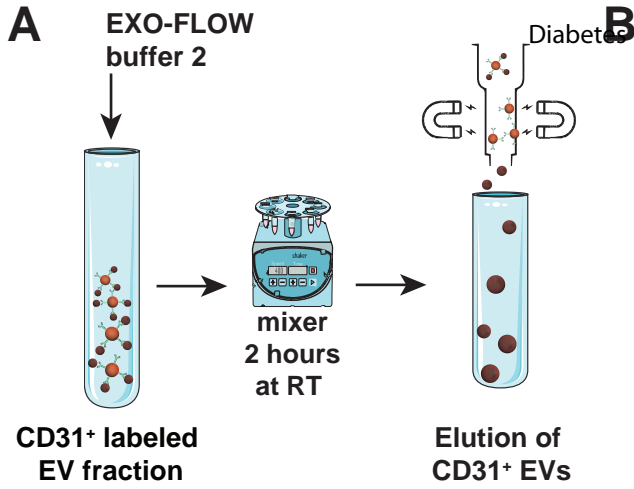
A

Age 41 of 53

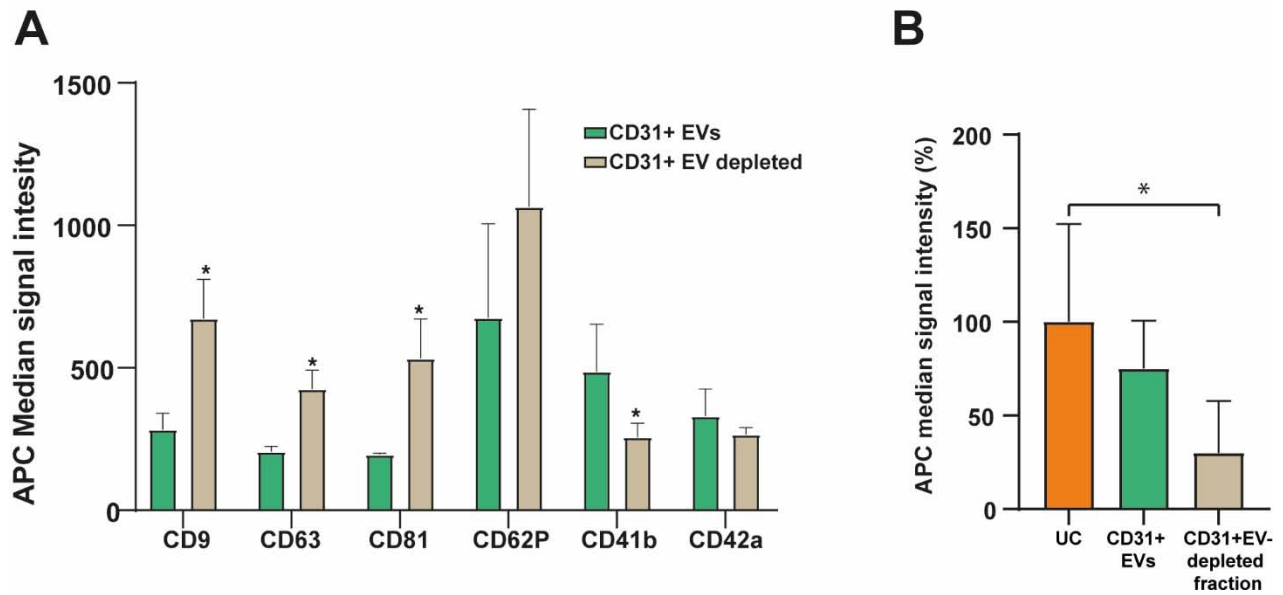


B





Supplementary Figure 1



A) Comparative cytofluorimetric detection of multiple markers in CD31+EVs vs CD31+ EV-depleted (n=3, from the same control plasma samples). * t test $p < 0.05$. **B)** Estimation of the yield of the isolation technique. Comparative cytofluorimetric detection of CD31 in EVs isolated with UC, in CD31+EVs, and the CD31+ depleted EVs (n=3, from the same control plasma samples). * ANOVA $p < 0.05$.

Supplementary Table 1. Literature supporting the selection of the miRNA panel.

| miRNA | References |
|--------------------|--|
| miR-126-3p | (Al-Kafaji et al., 2017; Amr et al., 2018; Jansen et al., 2016; Jansen et al., 2013; Liu et al., 2014; Meng et al., 2012; Mocharla et al., 2013; Olivieri et al., 2014; Olivieri et al., 2015b; Ortega et al., 2014; Rawal et al., 2017; Seyhan et al., 2016; Wang et al., 2014; Zampetaki et al., 2010; Zhang et al., 2017; Zhang et al., 2015; Zhang et al., 2013) |
| miR-146a-5p | (Alipoor et al., 2017; Baldeon et al., 2014; Garcia-Jacobo et al., 2019; Kong et al., 2011; Mensa et al., 2019; Radovic et al., 2018; Rong et al., 2013) |
| miR-155 | (Akhbari et al., 2019; Barutta et al., 2013; Beltrami et al., 2018; CorralFernandez et al., 2013; Huang et al., 2014; Liang et al., 2018a; Liang et al., 2018b; Mazloom et al., 2015; Moura et al., 2019; Tome-Carneiro et al., 2013; Wang et al., 2019; Wang et al., 2018; Yang et al., 2015) |
| miR-195-5p | (Marques et al., 2016) |
| miR-21-5p | (Chien et al., 2016; Ghorbani et al., 2018; Jansen et al., 2016; Jiang et al., 2017; La Sala et al., 2019; Liang et al., 2018b; Nunez Lopez et al., 2016; Olivieri et al., 2015a; Villard et al., 2015; Wang et al., 2014; Zampetaki et al., 2010; Zang et al., 2019) |
| miR-24-3p | (de Candia et al., 2017; Demirsoy et al., 2018; Kokkinopoulou et al., 2019; Prabu et al., 2019) |
| miR-320a | (Flowers et al., 2015; Villard et al., 2015) |
| miR-342-3p | (Assmann et al., 2018; Collares et al., 2013; de Candia et al., 2017) |
| miR-376a | (Joglekar et al., 2009) |
| miR-422a | (Latorre et al., 2017) |
| miR-451a | (Ding et al., 2016) |

- Akhbari, M., Khalili, M., Shahrabi-Farahani, M., Biglari, A., Bandarian, F., 2019. Expression Level of Circulating Cell Free miR-155 Gene in Serum of Patients with Diabetic Nephropathy. *Clin Lab* 65.
- Al-Kafaji, G., Al-Mahroos, G., Abdulla Al-Muhtareh, H., Sabry, M.A., Abdul Razzak, R., Salem, A.H., 2017. Circulating endothelium-enriched microRNA-126 as a potential biomarker for coronary artery disease in type 2 diabetes mellitus patients. *Biomarkers* 22, 268-278.
- Alipoor, B., Ghaedi, H., Meshkani, R., Torkamandi, S., Saffari, S., Iranpour, M., Omrani, M.D., 2017. Association of MiR-146a Expression and Type 2 Diabetes Mellitus: A Meta-Analysis. *Int J Mol Cell Med* 6, 156-163.
- Amr, K.S., Abdelmawgoud, H., Ali, Z.Y., Shehata, S., Raslan, H.M., 2018. Potential value of circulating microRNA126 and microRNA-210 as biomarkers for type 2 diabetes with coronary artery disease. *Br J Biomed Sci* 75, 82-87.
- Assmann, T.S., Recamonde-Mendoza, M., de Souza, B.M., Bauer, A.C., Crispim, D., 2018. MicroRNAs and diabetic kidney disease: Systematic review and bioinformatic analysis. *Mol Cell Endocrinol* 477, 90-102.
- Baldeon, R.L., Weigelt, K., de Wit, H., Ozcan, B., van Oudenaren, A., Sempertegui, F., Sijbrands, E., Grosse, L., Freire, W., Drexhage, H.A., Leenen, P.J., 2014. Decreased serum level of miR-146a as sign of chronic inflammation in type 2 diabetic patients. *PLoS One* 9, e115209.
- Barutta, F., Tricarico, M., Corbelli, A., Annaratone, L., Pinach, S., Grimaldi, S., Bruno, G., Cimino, D., Taverna, D., Deregibus, M.C., Rastaldi, M.P., Perin, P.C., Gruden, G., 2013. Urinary exosomal microRNAs in incipient diabetic nephropathy. *PLoS One* 8, e73798.

- Beltrami, C., Simpson, K., Jesky, M., Wonnacott, A., Carrington, C., Holmans, P., Newbury, L., Jenkins, R., Ashdown, T., Dayan, C., Satchell, S., Corish, P., Cockwell, P., Fraser, D., Bowen, T., 2018. Association of Elevated Urinary miR-126, miR-155, and miR-29b with Diabetic Kidney Disease. *Am J Pathol* 188, 1982-1992.
- Chien, H.Y., Chen, C.Y., Chiu, Y.H., Lin, Y.C., Li, W.C., 2016. Differential microRNA Profiles Predict Diabetic Nephropathy Progression in Taiwan. *Int J Med Sci* 13, 457-465.
- Collares, C.V., Evangelista, A.F., Xavier, D.J., Rassi, D.M., Arns, T., Foss-Freitas, M.C., Foss, M.C., Puthier, D., Sakamoto-Hojo, E.T., Passos, G.A., Donadi, E.A., 2013. Identifying common and specific microRNAs expressed in peripheral blood mononuclear cell of type 1, type 2, and gestational diabetes mellitus patients. *BMC Res Notes* 6, 491.
- Corral-Fernandez, N.E., Salgado-Bustamante, M., Martinez-Leija, M.E., Cortez-Espinosa, N., Garcia-Hernandez, M.H., Reynaga-Hernandez, E., Quezada-Calvillo, R., Portales-Perez, D.P., 2013. Dysregulated miR-155 expression in peripheral blood mononuclear cells from patients with type 2 diabetes. *Exp Clin Endocrinol Diabetes* 121, 347-353.
- de Candia, P., Spinetti, G., Specchia, C., Sangalli, E., La Sala, L., Uccellatore, A., Lupini, S., Genovese, S., Matarese, G., Ceriello, A., 2017. A unique plasma microRNA profile defines type 2 diabetes progression. *PLoS One* 12, e0188980.
- Demirsoy, I.H., Ertural, D.Y., Balci, S., Cinkir, U., Sezer, K., Tamer, L., Aras, N., 2018. Profiles of Circulating MiRNAs Following Metformin Treatment in Patients with Type 2 Diabetes. *J Med Biochem* 37, 499-506.
- Ding, L., Ai, D., Wu, R., Zhang, T., Jing, L., Lu, J., Zhong, L., 2016. Identification of the differential expression of serum microRNA in type 2 diabetes. *Biosci Biotechnol Biochem* 80, 461-465.
- Flowers, E., Aouizerat, B.E., Abbasi, F., Lamendola, C., Grove, K.M., Fukuoka, Y., Reaven, G.M., 2015. Circulating microRNA-320a and microRNA-486 predict thiazolidinedione response: Moving towards precision health for diabetes prevention. *Metabolism* 64, 1051-1059.
- Garcia-Jacobo, R.E., Uresti-Rivera, E.E., Portales-Perez, D.P., Gonzalez-Amaro, R., Lara-Ramirez, E.E., EncisoMoreno, J.A., Garcia-Hernandez, M.H., 2019. Circulating miR-146a, miR-34a and miR-375 in type 2 diabetes patients, pre-diabetic and normal-glycaemic individuals in relation to beta-cell function, insulin resistance and metabolic parameters. *Clin Exp Pharmacol Physiol* 46, 1092-1100.
- Ghorbani, S., Mahdavi, R., Alipoor, B., Panahi, G., Nasli Esfahani, E., Razi, F., Taghikhani, M., Meshkani, R., 2018. Decreased serum microRNA-21 level is associated with obesity in healthy and type 2 diabetic subjects. *Arch Physiol Biochem* 124, 300-305.
- Huang, Y., Liu, Y., Li, L., Su, B., Yang, L., Fan, W., Yin, Q., Chen, L., Cui, T., Zhang, J., Lu, Y., Cheng, J., Fu, P., Liu, F., 2014. Involvement of inflammation-related miR-155 and miR-146a in diabetic nephropathy: implications for glomerular endothelial injury. *BMC Nephrol* 15, 142.
- Jansen, F., Wang, H., Przybilla, D., Franklin, B.S., Dolf, A., Pfeifer, P., Schmitz, T., Flender, A., Endl, E., Nickenig, G., Werner, N., 2016. Vascular endothelial microparticles-incorporated microRNAs are altered in patients with diabetes mellitus. *Cardiovasc Diabetol* 15, 49.
- Jansen, F., Yang, X., Hoelscher, M., Cattelan, A., Schmitz, T., Proebsting, S., Wenzel, D., Vosen, S., Franklin, B.S., Fleischmann, B.K., Nickenig, G., Werner, N., 2013. Endothelial microparticle-mediated transfer of MicroRNA-126 promotes vascular endothelial cell repair via SPRED1 and is abrogated in glucose-damaged endothelial microparticles. *Circulation* 128, 2026-2038.
- Jiang, Q., Lyu, X.M., Yuan, Y., Wang, L., 2017. Plasma miR-21 expression: an indicator for the severity of Type 2 diabetes with diabetic retinopathy. *Biosci Rep* 37.
- Joglekar, M.V., Joglekar, V.M., Hardikar, A.A., 2009. Expression of islet-specific microRNAs during human pancreatic development. *Gene Expr Patterns* 9, 109-113.
- Kokkinopoulou, I., Maratou, E., Mitrou, P., Boutati, E., Sideris, D.C., Fragoulis, E.G., Christodoulou, M.I., 2019. Decreased expression of microRNAs targeting type-2 diabetes susceptibility genes in peripheral blood of patients and predisposed individuals. *Endocrine* 66, 226-239.
- Kong, L., Zhu, J., Han, W., Jiang, X., Xu, M., Zhao, Y., Dong, Q., Pang, Z., Guan, Q., Gao, L., Zhao, J., Zhao, L., 2011. Significance of serum microRNAs in pre-diabetes and newly diagnosed type 2 diabetes: a clinical study. *Acta Diabetol* 48, 61-69.
- La Sala, L., Mrakic-Sposta, S., Tagliabue, E., Prattichizzo, F., Micheloni, S., Sangalli, E., Specchia, C., Uccellatore, A.C., Lupini, S., Spinetti, G., de Candia, P., Ceriello, A., 2019. Circulating microRNA-21 is an early predictor of ROS-mediated damage in subjects with high risk of developing diabetes and in drug-naive T2D. *Cardiovasc Diabetol* 18, 18.
- Latorre, J., Moreno-Navarrete, J.M., Mercader, J.M., Sabater, M., Rovira, O., Girones, J., Ricart, W., Fernandez-Real, J.M., Ortega, F.J., 2017. Decreased lipid metabolism but increased FA biosynthesis are coupled with changes in liver microRNAs in obese subjects with NAFLD. *Int J Obes (Lond)* 41, 620-630.
- Liang, Y.Z., Dong, J., Zhang, J., Wang, S., He, Y., Yan, Y.X., 2018a. Identification of Neuroendocrine Stress Response-Related Circulating MicroRNAs as Biomarkers for Type 2 Diabetes Mellitus and Insulin Resistance. *Front Endocrinol (Lausanne)* 9, 132.
- Liang, Y.Z., Li, J.J., Xiao, H.B., He, Y., Zhang, L., Yan, Y.X., 2018b. Identification of stress-related microRNA biomarkers in type 2 diabetes mellitus: A systematic review and meta-analysis. *J Diabetes*.

- Liu, Y., Gao, G., Yang, C., Zhou, K., Shen, B., Liang, H., Jiang, X., 2014. The role of circulating microRNA-126 (miR126): a novel biomarker for screening prediabetes and newly diagnosed type 2 diabetes mellitus. *Int J Mol Sci* 15, 10567-10577.
- Marques, F.Z., Vizi, D., Khammy, O., Mariani, J.A., Kaye, D.M., 2016. The transcardiac gradient of cardiomiRNAs in the failing heart. *Eur J Heart Fail* 18, 1000-1008.
- Mazloom, H., Alizadeh, S., Pasalar, P., Esfahani, E.N., Meshkani, R., 2015. Downregulated microRNA-155 expression in peripheral blood mononuclear cells of type 2 diabetic patients is not correlated with increased inflammatory cytokine production. *Cytokine* 76, 403-408.
- Meng, S., Cao, J.T., Zhang, B., Zhou, Q., Shen, C.X., Wang, C.Q., 2012. Downregulation of microRNA-126 in endothelial progenitor cells from diabetes patients, impairs their functional properties, via target gene Spred-1. *J Mol Cell Cardiol* 53, 64-72.
- Mensa, E., Giuliani, A., Matakchione, G., Gurau, F., Bonfigli, A.R., Romagnoli, F., De Luca, M., Sabbatinelli, J., Olivieri, F., 2019. Circulating miR-146a in healthy aging and type 2 diabetes: Age- and gender-specific trajectories. *Mech Ageing Dev* 180, 1-10.
- Mocharla, P., Briand, S., Giannotti, G., Dorries, C., Jakob, P., Paneni, F., Luscher, T., Landmesser, U., 2013. AngiomiR-126 expression and secretion from circulating CD34(+) and CD14(+) PBMCs: role for proangiogenic effects and alterations in type 2 diabetics. *Blood* 121, 226-236.
- Moura, J., Sorensen, A., Leal, E.C., Svendsen, R., Carvalho, L., Willemoes, R.J., Jorgensen, P.T., Jenssen, H., Wengel, J., Dalgaard, L.T., Carvalho, E., 2019. microRNA-155 inhibition restores Fibroblast Growth Factor 7 expression in diabetic skin and decreases wound inflammation. *Sci Rep* 9, 5836.
- Nunez Lopez, Y.O., Garufi, G., Seyhan, A.A., 2016. Altered levels of circulating cytokines and microRNAs in lean and obese individuals with prediabetes and type 2 diabetes. *Mol Biosyst* 13, 106-121.
- Olivieri, F., Bonafe, M., Spazzafumo, L., Gobbi, M., Prattichizzo, F., Recchioni, R., Marcheselli, F., La Sala, L., Galeazzi, R., Rippo, M.R., Fulgenzi, G., Angelini, S., Lazzarini, R., Bonfigli, A.R., Bruge, F., Tiano, L., Genovese, S., Ceriello, A., Boemi, M., Franceschi, C., Procopio, A.D., Testa, R., 2014. Age- and glycemia-related miR-126-3p levels in plasma and endothelial cells. *Aging (Albany NY)* 6, 771-787.
- Olivieri, F., Spazzafumo, L., Bonafe, M., Recchioni, R., Prattichizzo, F., Marcheselli, F., Micolucci, L., Mensa, E., Giuliani, A., Santini, G., Gobbi, M., Lazzarini, R., Boemi, M., Testa, R., Antonicelli, R., Procopio, A.D., Bonfigli, A.R., 2015a. MiR-21-5p and miR-126a-3p levels in plasma and circulating angiogenic cells: relationship with type 2 diabetes complications. *Oncotarget* 6, 35372-35382.
- Olivieri, F., Spazzafumo, L., Bonafè, M., Recchioni, R., Prattichizzo, F., Marcheselli, F., Micolucci, L., Mensà, E., Giuliani, A., Santini, G., Gobbi, M., Lazzarini, R., Boemi, M., Testa, R., Antonicelli, R., Procopio, A.D., Bonfigli, A.R., 2015b. MiR-21-5p and miR-126a-3p levels in plasma and circulating angiogenic cells: Relationship with type 2 diabetes complications. *Oncotarget* 6, 35372-35382.
- Ortega, F.J., Mercader, J.M., Moreno-Navarrete, J.M., Rovira, O., Guerra, E., Esteve, E., Xifra, G., Martinez, C., Ricart, W., Rieusset, J., Rome, S., Karczewska-Kupczewska, M., Strackowski, M., Fernandez-Real, J.M., 2014. Profiling of circulating microRNAs reveals common microRNAs linked to type 2 diabetes that change with insulin sensitization. *Diabetes Care* 37, 1375-1383.
- Prabu, P., Rome, S., Sathishkumar, C., Gastebois, C., Meugnier, E., Mohan, V., Balasubramanyam, M., 2019. MicroRNAs from urinary extracellular vesicles are non-invasive early biomarkers of diabetic nephropathy in type 2 diabetes patients with the 'Asian Indian phenotype'. *Diabetes Metab* 45, 276-285.
- Radovic, N., Nikolic Jakoba, N., Petrovic, N., Milosavljevic, A., Brkovic, B., Roganovic, J., 2018. MicroRNA-146a and microRNA-155 as novel crevicular fluid biomarkers for periodontitis in non-diabetic and type 2 diabetic patients. *J Clin Periodontol* 45, 663-671.
- Rawal, S., Munasinghe, P.E., Shindikar, A., Paulin, J., Cameron, V., Manning, P., Williams, M.J., Jones, G.T., Bunton, R., Galvin, I., Katare, R., 2017. Down-regulation of proangiogenic microRNA-126 and microRNA-132 are early modulators of diabetic cardiac microangiopathy. *Cardiovasc Res* 113, 90-101.
- Rong, Y., Bao, W., Shan, Z., Liu, J., Yu, X., Xia, S., Gao, H., Wang, X., Yao, P., Hu, F.B., Liu, L., 2013. Increased microRNA-146a levels in plasma of patients with newly diagnosed type 2 diabetes mellitus. *PLoS One* 8, e73272.
- Seyhan, A.A., Nunez Lopez, Y.O., Xie, H., Yi, F., Mathews, C., Pasarica, M., Pratley, R.E., 2016. Pancreas-enriched miRNAs are altered in the circulation of subjects with diabetes: a pilot cross-sectional study. *Sci Rep* 6, 31479.
- Tome-Carneiro, J., Larrosa, M., Yanez-Gascon, M.J., Davalos, A., Gil-Zamorano, J., Gonzalez, M., Garcia-Almagro, F.J., Ruiz Ros, J.A., Tomas-Barberan, F.A., Espin, J.C., Garcia-Conesa, M.T., 2013. One-year supplementation with a grape extract containing resveratrol modulates inflammatory-related microRNAs and cytokines expression in peripheral blood mononuclear cells of type 2 diabetes and hypertensive patients with coronary artery disease. *Pharmacol Res* 72, 69-82.
- Villard, A., Marchand, L., Thivolet, C., Rome, S., 2015. Diagnostic Value of Cell-free Circulating MicroRNAs for Obesity and Type 2 Diabetes: A Meta-analysis. *J Mol Biomark Diagn* 6.
- Wang, J., Wang, G., Liang, Y., Zhou, X., 2019. Expression Profiling and Clinical Significance of Plasma MicroRNAs in Diabetic Nephropathy. *J Diabetes Res* 2019, 5204394.
- Wang, X., Sundquist, J., Zoller, B., Memon, A.A., Palmer, K., Sundquist, K., Bennet, L., 2014. Determination of 14 circulating microRNAs in Swedes and Iraqis with and without diabetes mellitus type 2. *PLoS One* 9, e86792.

- Wang, Y., Zheng, Z.J., Jia, Y.J., Yang, Y.L., Xue, Y.M., 2018. Role of p53/miR-155-5p/sirt1 loop in renal tubular injury of diabetic kidney disease. *J Transl Med* 16, 146.
- Yang, T.T., Song, S.J., Xue, H.B., Shi, D.F., Liu, C.M., Liu, H., 2015. Regulatory T cells in the pathogenesis of type 2 diabetes mellitus retinopathy by miR-155. *Eur Rev Med Pharmacol Sci* 19, 2010-2015.
- Zampetaki, A., Kiechl, S., Drozdov, I., Willeit, P., Mayr, U., Prokopi, M., Mayr, A., Weger, S., Oberhollenzer, F., Bonora, E., Shah, A., Willeit, J., Mayr, M., 2010. Plasma microRNA profiling reveals loss of endothelial miR126 and other microRNAs in type 2 diabetes. *Circ Res* 107, 810-817.
- Zang, J., Maxwell, A.P., Simpson, D.A., McKay, G.J., 2019. Differential Expression of Urinary Exosomal MicroRNAs miR-21-5p and miR-30b-5p in Individuals with Diabetic Kidney Disease. *Sci Rep* 9, 10900.
- Zhang, J., Sun, X.J., Chen, J., Hu, Z.W., Wang, L., Gu, D.M., Wang, A.P., 2017. Increasing the miR-126 expression in the peripheral blood of patients with diabetic foot ulcers treated with maggot debridement therapy. *J Diabetes Complications* 31, 241-244.
- Zhang, T., Li, L., Shang, Q., Lv, C., Wang, C., Su, B., 2015. Circulating miR-126 is a potential biomarker to predict the onset of type 2 diabetes mellitus in susceptible individuals. *Biochem Biophys Res Commun* 463, 60-63.
- Zhang, T., Lv, C., Li, L., Chen, S., Liu, S., Wang, C., Su, B., 2013. Plasma miR-126 is a potential biomarker for early prediction of type 2 diabetes mellitus in susceptible individuals. *Biomed Res Int* 2013, 761617.

Supplementary Table 2. Comparison of CD31⁺EV-shuttled miRNA relative expression among CTRL, T2DM-NC, and T2DM-C subjects. Variables are expressed as median (interquartile range). P value from Mann-Whitney *U* test for CTRL vs. T2DM and from Kruskal-Wallis test for CTRL vs. T2DM-NC vs. T2DM-C.

| miRNA | CTR | T2DM-C | T2DM-NC | p value (CTR vs. T2DM) | p value (CTR vs. T2DM-NC vs. T2DM-C) |
|--------------------|---------------|---------------|----------------|---------------------------------------|---|
| miR-126-3p | 36.5 (44.4) | 18.5 (21.0) | 22.9 (34.7) | <0.001 | <0.001 |
| miR-146a-5p | 0.4 (0.7) | 1.7 (8.2) | 30.8 (206.9) | <0.001 | <0.001 |
| miR-155 | 739.8 (677.1) | 1.1 (1.2) | 0.1 (0.9) | <0.001 | <0.001 |
| miR-195-5p | 89.2 (60.4) | 7.8 (7.1) | 1.1 (7.9) | <0.001 | <0.001 |
| miR-21-5p | 62.9 (100.4) | 138.2 (127.5) | 249.6 (156.8) | <0.001 | <0.001 |
| miR-24-3p | 71.3 (109.2) | 10.3 (8.8) | 0.9 (6.1) | <0.001 | <0.001 |
| miR-320a | 53.2 (110.9) | 49.5 (83.5) | 22.7 (37.9) | <0.001 | <0.001 |
| miR-342-3p | 0.2 (0.2) | 0.4 (0.5) | 1.4 (2.5) | <0.001 | <0.001 |
| miR-376a | 23.9 (146.9) | 20.4 (46.2) | 22.5 (150.6) | 0.212 | 0.362 |
| miR-422a | 0.3 (0.6) | 4.0 (7.4) | 10.7 (8.2) | <0.001 | <0.001 |
| miR-451a | 0.3 (0.3) | 0.6 (0.7) | 1.6 (1.5) | <0.001 | <0.001 |

Supplementary Table 3. Binary logistic regression analysis of miRNAs associated with the presence of complications in T2DM patients. Odds ratio (95% CI) are expressed per 0.5 SD increase of each miRNA.

| miRNA | B | SE | P value | OR (95% CI) |
|--------------|----------|-----------|----------------|-----------------------|
| miR-146a-5p | 0.693 | 0.343 | 0.043 | 1.999 (1.021 – 3.914) |
| miR-320a | -0.446 | 0.130 | 0.001 | 0.640 (0.496 – 0.826) |
| miR-422a | 0.292 | 0.141 | 0.038 | 1.339 (1.016 – 1.763) |
| miR-451a | 0.401 | 0.142 | 0.005 | 1.493 (1.131 – 1.973) |

Supplementary Table 4. Binary logistic regression analysis of miRNAs associated with the presence of complications in T2DM patients. BMI and LDL-C were included into the model as covariates. Odds ratio (95% CI) are expressed per 0.5 SD increase of each miRNA.

| miRNA | B | SE | P value | OR (95% CI) |
|--------------|----------|-----------|----------------|------------------------|
| miR-146a-5p | 1.208 | 0.632 | 0.056 | 3.348 (0.969 – 11.563) |
| miR-320a | -0.874 | 0.268 | 0.001 | 0.417 (0.247 – 0.705) |
| miR-422a | 0.616 | 0.304 | 0.043 | 1.852 (1.021 – 3.359) |
| miR-451a | 0.804 | 0.304 | 0.008 | 2.235 (1.232 – 4.053) |
| BMI | -0.040 | 0.045 | 0.371 | 0.961 (0.880 – 1.049) |
| LDL-C | -0.015 | 0.006 | 0.023 | 0.986 (0.973 – 0.998) |

Supplementary Table 5. Comparison of CD31⁺-EV miRNA levels in T2DM individuals according to the presence of specific complications after adjustment for age and gender. In the case of MACE, comparisons after adjustment also for HbA1c and the presence of any other T2DM complication are also reported. P values of the comparison of the estimated marginal means are reported. Differences of the adjusted mean relative expressions between complication present and absent are reported where $p < 0.05$.

| miRNAs | At least one complication (n=101) | Neuropathy (n=28) | Nephropathy (n=20) | Retinopathy (n=48) | Peripheral artery disease (n=22) | MACE adj. for age and gender (n=52) | MACE adj. for age, gender, HbA1c, other complications (n=52) |
|-------------|-----------------------------------|-------------------|--------------------|--------------------|----------------------------------|-------------------------------------|--|
| miR-126-3p | 0.214 | 0.166 | 0.693 | 0.309 | 0.312 | 0.213 | 0.949 |
| miR-146a-5p | 0.002 (125.6) | 0.107 | 0.318 | 0.205 | 0.020 (124.5) | <0.001 (201.2) | <0.001 (204.8) |
| miR-155 | <0.001 (-0.6) | 0.192 | 0.980 | 0.542 | 0.013 (-0.45) | <0.001 (-1.1) | <0.001 (-1.0) |
| miR-195-5p | <0.001 (-5.3) | 0.372 | 0.606 | 0.713 | 0.016 (-4.0) | <0.001 (-7.4) | 0.002 (-5.7) |
| miR-21-5p | <0.001 (103.6) | 0.903 | 0.538 | 0.522 | 0.970 | <0.001 (131.2) | <0.001 (124.0) |
| miR-24-3p | <0.001 (-7.7) | 0.168 | 0.175 | 0.497 | 0.008 (-4.8) | <0.001 (-9.8) | <0.001 (-7.3) |
| miR-320a | 0.057 | 0.364 | 0.258 | 0.735 | 0.042 (-38.1) | 0.065 | 0.962 |
| miR-342-3p | <0.001 (1.2) | 0.656 | 0.834 | 0.302 | 0.111 | <0.001 (1.6) | <0.001 (1.5) |
| miR-376a | 0.056 | 0.900 | 0.519 | 0.707 | 0.745 | <0.001 (97.0) | <0.001 (92.6) |
| miR-422a | <0.001 (5.2) | 0.685 | 0.737 | 0.517 | 0.064 | <0.001 (6.2) | <0.001 (5.6) |
| miR-451a | <0.001 (0.8) | 0.686 | 0.321 | 0.466 | 0.337 | <0.001 (1.2) | <0.001 (1.3) |

Supplementary Table 6. Complete correlation matrix of Pearson's correlations between 11 CD31⁺EV miRNAs and selected clinical and biochemical variables.

| Variables | | miR-126-3p | miR-146a-5p | miR-155 | miR-195-5p | miR-21-5p | miR-24-3p | miR-320a | miR-342-3p | miR-376a | miR-422a | miR-451a |
|------------------------|----------|------------|-------------|---------|------------|-----------|-----------|----------|------------|----------|----------|----------|
| Age | r | -0.026 | 0.149 | -0.318 | -0.415 | 0.252 | -0.270 | -0.084 | 0.224 | 0.039 | 0.301 | 0.281 |
| | p | 0.706 | 0.028 | <0.001 | <0.001 | <0.001 | <0.001 | 0.217 | <0.001 | 0.567 | <0.001 | <0.001 |
| BMI | r | 0.007 | 0.096 | -0.151 | -0.176 | 0.138 | -0.147 | 0.035 | 0.105 | 0.023 | 0.209 | 0.146 |
| | p | 0.920 | 0.160 | 0.026 | 0.009 | 0.043 | 0.030 | 0.603 | 0.121 | 0.733 | 0.002 | 0.032 |
| Waist/hip ratio | r | -0.084 | 0.340 | -0.217 | -0.288 | 0.252 | -0.224 | -0.016 | 0.290 | 0.015 | 0.346 | 0.308 |
| | p | 0.217 | <0.001 | 0.001 | <0.001 | <0.001 | <0.001 | 0.813 | <0.001 | 0.827 | <0.001 | <0.001 |
| Fasting glucose | r | -0.162 | 0.163 | -0.445 | -0.513 | 0.281 | -0.423 | -0.170 | 0.272 | -0.001 | 0.403 | 0.269 |
| | p | 0.017 | 0.016 | <0.001 | <0.001 | <0.001 | <0.001 | 0.012 | <0.001 | 0.988 | <0.001 | <0.001 |
| HbA1C | r | -0.086 | 0.173 | -0.398 | -0.475 | 0.271 | -0.386 | -0.122 | 0.295 | 0.055 | 0.382 | 0.286 |
| | p | 0.208 | 0.010 | <0.001 | <0.001 | <0.001 | <0.001 | 0.073 | <0.001 | 0.418 | <0.001 | <0.001 |
| Fasting insulin | r | -0.082 | -0.012 | -0.100 | -0.095 | 0.012 | -0.082 | 0.006 | 0.002 | -0.021 | -0.012 | 0.001 |
| | p | 0.229 | 0.855 | 0.140 | 0.162 | 0.858 | 0.225 | 0.929 | 0.976 | 0.756 | 0.860 | 0.985 |
| HOMA index | r | -0.107 | 0.014 | -0.176 | -0.182 | 0.053 | -0.157 | -0.046 | 0.053 | -0.022 | 0.056 | 0.046 |
| | p | 0.116 | 0.841 | 0.009 | 0.007 | 0.433 | 0.020 | 0.495 | 0.434 | 0.748 | 0.411 | 0.502 |
| Azotemia | r | 0.095 | 0.106 | -0.100 | -0.107 | 0.241 | -0.101 | 0.153 | 0.280 | 0.126 | 0.152 | 0.390 |
| | p | 0.163 | 0.118 | 0.141 | 0.114 | <0.001 | 0.136 | 0.024 | <0.001 | 0.063 | 0.025 | <0.001 |
| Creatinine | r | 0.078 | 0.206 | -0.133 | -0.197 | 0.310 | -0.176 | 0.129 | 0.344 | 0.077 | 0.219 | 0.384 |
| | p | 0.250 | 0.002 | 0.049 | 0.003 | <0.001 | 0.009 | 0.057 | <0.001 | 0.257 | 0.001 | <0.001 |
| eGFR | r | -0.075 | -0.119 | 0.080 | 0.138 | -0.148 | 0.088 | -0.003 | -0.184 | -0.088 | -0.145 | -0.198 |
| | p | 0.273 | 0.078 | 0.242 | 0.042 | 0.029 | 0.195 | 0.969 | 0.006 | 0.193 | 0.032 | 0.003 |
| Uric acid | r | 0.045 | 0.143 | -0.060 | -0.100 | 0.119 | -0.081 | -0.028 | 0.171 | -0.005 | 0.107 | 0.082 |
| | p | 0.509 | 0.035 | 0.382 | 0.143 | 0.079 | 0.233 | 0.681 | 0.011 | 0.947 | 0.115 | 0.230 |
| ALT | r | -0.054 | 0.016 | -0.069 | -0.051 | -0.044 | -0.052 | 0.013 | 0.043 | -0.089 | 0.150 | -0.098 |
| | p | 0.429 | 0.816 | 0.310 | 0.452 | 0.522 | 0.448 | 0.851 | 0.527 | 0.190 | 0.027 | 0.148 |
| AST | r | -0.105 | 0.011 | -0.075 | -0.067 | -0.004 | -0.096 | -0.060 | 0.050 | -0.053 | 0.152 | -0.064 |
| | p | 0.124 | 0.873 | 0.273 | 0.326 | 0.957 | 0.160 | 0.378 | 0.460 | 0.439 | 0.025 | 0.347 |
| Gamma GT | r | -0.114 | -0.007 | -0.143 | -0.149 | 0.046 | -0.125 | -0.150 | 0.126 | -0.114 | 0.144 | 0.019 |
| | p | 0.094 | 0.919 | 0.034 | 0.028 | 0.498 | 0.065 | 0.027 | 0.063 | 0.092 | 0.034 | 0.778 |
| Total bilirubin | r | -0.019 | -0.036 | 0.071 | 0.097 | -0.026 | 0.009 | -0.054 | 0.016 | -0.021 | 0.030 | -0.023 |
| | p | 0.782 | 0.595 | 0.294 | 0.152 | 0.705 | 0.893 | 0.428 | 0.813 | 0.754 | 0.657 | 0.734 |

| Variables | | miR-126-3p | miR-146a-5p | miR-155 | miR-195-5p | miR-21-5p | miR-24-3p | miR-320a | miR-342-3p | miR-376a | miR-422a | miR-451a |
|--------------------------|----------|------------|-------------|---------|------------|-----------|-----------|----------|------------|----------|----------|----------|
| WBC | r | 0.037 | 0.138 | -0.088 | -0.162 | 0.127 | -0.153 | -0.114 | 0.205 | 0.001 | 0.165 | 0.155 |
| | p | 0.586 | 0.042 | 0.196 | 0.017 | 0.061 | 0.023 | 0.094 | 0.002 | 0.983 | 0.015 | 0.022 |
| RBC | r | -0.066 | 0.056 | -0.181 | -0.169 | 0.053 | -0.199 | -0.163 | 0.019 | 0.032 | 0.117 | 0.048 |
| | p | 0.334 | 0.414 | 0.007 | 0.012 | 0.432 | 0.003 | 0.016 | 0.783 | 0.638 | 0.085 | 0.478 |
| Hemoglobin | r | -0.103 | 0.034 | -0.165 | -0.167 | 0.078 | -0.173 | -0.123 | 0.026 | -0.001 | 0.095 | 0.011 |
| | p | 0.129 | 0.619 | 0.015 | 0.013 | 0.254 | 0.010 | 0.070 | 0.704 | 0.989 | 0.162 | 0.869 |
| Hematocrit | r | -0.082 | 0.064 | -0.177 | -0.191 | 0.063 | -0.182 | -0.117 | 0.040 | 0.014 | 0.106 | 0.032 |
| | p | 0.226 | 0.344 | 0.009 | 0.005 | 0.352 | 0.007 | 0.084 | 0.552 | 0.842 | 0.119 | 0.643 |
| Serum iron | r | -0.086 | -0.062 | -0.025 | -0.017 | 0.021 | -0.029 | -0.157 | 0.023 | -0.030 | 0.022 | -0.050 |
| | p | 0.206 | 0.363 | 0.714 | 0.803 | 0.753 | 0.667 | 0.020 | 0.736 | 0.661 | 0.750 | 0.467 |
| Transferrin | r | -0.106 | 0.012 | -0.134 | -0.091 | 0.047 | -0.007 | 0.011 | 0.089 | -0.095 | 0.084 | 0.055 |
| | p | 0.119 | 0.862 | 0.048 | 0.182 | 0.490 | 0.915 | 0.875 | 0.192 | 0.163 | 0.218 | 0.419 |
| Ferritin | r | -0.086 | -0.025 | -0.007 | -0.014 | 0.039 | -0.094 | -0.080 | 0.115 | -0.078 | 0.073 | -0.031 |
| | p | 0.204 | 0.715 | 0.923 | 0.837 | 0.569 | 0.168 | 0.238 | 0.091 | 0.254 | 0.282 | 0.653 |
| Platelets | r | 0.028 | -0.028 | 0.096 | 0.087 | -0.146 | 0.121 | 0.021 | -0.121 | -0.077 | -0.081 | -0.065 |
| | p | 0.684 | 0.681 | 0.159 | 0.199 | 0.031 | 0.074 | 0.754 | 0.074 | 0.255 | 0.234 | 0.342 |
| Total cholesterol | r | 0.109 | -0.197 | 0.109 | 0.159 | -0.175 | 0.171 | -0.005 | -0.214 | -0.115 | -0.239 | -0.210 |
| | p | 0.108 | 0.003 | 0.110 | 0.019 | 0.010 | 0.012 | 0.943 | 0.001 | 0.090 | <0.001 | 0.002 |
| HDL-cholesterol | r | 0.036 | -0.181 | 0.247 | 0.314 | -0.273 | 0.299 | 0.052 | -0.243 | -0.058 | -0.343 | -0.250 |
| | p | 0.596 | 0.007 | <0.001 | <0.001 | <0.001 | <0.001 | 0.444 | <0.001 | 0.395 | <0.001 | <0.001 |
| LDL-cholesterol | r | 0.066 | -0.235 | 0.104 | 0.168 | -0.162 | 0.169 | -0.010 | -0.269 | -0.054 | -0.247 | -0.222 |
| | p | 0.334 | <0.001 | 0.126 | 0.013 | 0.017 | 0.012 | 0.888 | <0.001 | 0.432 | <0.001 | <0.001 |
| ApoA1 | r | 0.056 | -0.175 | 0.197 | 0.296 | -0.234 | 0.293 | 0.033 | -0.203 | -0.014 | -0.319 | -0.202 |
| | p | 0.408 | 0.009 | 0.003 | <0.001 | <0.001 | <0.001 | 0.626 | 0.003 | 0.832 | <0.001 | 0.003 |
| ApoB | r | 0.119 | -0.124 | 0.078 | 0.156 | -0.074 | 0.131 | 0.015 | -0.161 | -0.016 | -0.190 | -0.108 |
| | p | 0.080 | 0.068 | 0.254 | 0.021 | 0.278 | 0.054 | 0.826 | 0.017 | 0.812 | 0.005 | 0.112 |
| Triglycerides | r | -0.016 | 0.109 | -0.112 | -0.127 | 0.051 | -0.114 | -0.028 | 0.156 | -0.096 | 0.162 | 0.049 |
| | p | 0.809 | 0.110 | 0.099 | 0.062 | 0.452 | 0.092 | 0.678 | 0.021 | 0.156 | 0.017 | 0.471 |
| hs-CRP | r | -0.044 | 0.180 | -0.085 | -0.115 | 0.055 | -0.094 | -0.039 | 0.131 | 0.059 | 0.141 | 0.009 |
| | p | 0.515 | 0.688 | 0.213 | 0.089 | 0.422 | 0.165 | 0.567 | 0.054 | 0.383 | 0.038 | 0.895 |
| Fibrinogen | r | 0.152 | 0.070 | -0.057 | -0.086 | 0.129 | -0.097 | 0.047 | 0.208 | -0.032 | 0.206 | 0.228 |
| | p | 0.034 | 0.329 | 0.426 | 0.230 | 0.072 | 0.177 | 0.510 | 0.004 | 0.652 | 0.004 | 0.001 |

| Variables | | miR-126-3p | miR-146a-5p | miR-155 | miR-195-5p | miR-21-5p | miR-24-3p | miR-320a | miR-342-3p | miR-376a | miR-422a | miR-451a |
|------------------------|----------|------------|-------------|---------|------------|-----------|-----------|----------|------------|----------|----------|----------|
| PAI-1 | r | -0.057 | 0.022 | -0.088 | -0.138 | -0.071 | -0.086 | -0.028 | -0.010 | -0.066 | -0.008 | -0.043 |
| | p | 0.404 | 0.744 | 0.194 | 0.041 | 0.299 | 0.207 | 0.681 | 0.889 | 0.334 | 0.901 | 0.532 |
| Total proteins | r | -0.052 | 0.034 | -0.130 | -0.162 | 0.077 | -0.167 | -0.132 | 0.179 | -0.048 | 0.273 | 0.107 |
| | p | 0.441 | 0.620 | 0.056 | 0.017 | 0.260 | 0.013 | 0.051 | 0.008 | 0.480 | <0.001 | 0.115 |
| Telomere length | r | -0.021 | -0.221 | 0.123 | 0.154 | -0.185 | 0.111 | 0.005 | -0.295 | -0.031 | -0.216 | -0.200 |
| | p | 0.755 | 0.001 | 0.073 | 0.025 | 0.007 | 0.106 | 0.948 | <0.001 | 0.651 | 0.002 | 0.003 |
| miR-126-3p | r | 1.000 | 0.098 | 0.222 | 0.313 | 0.079 | 0.143 | 0.169 | 0.110 | -0.053 | -0.016 | 0.143 |
| | p | NA | 0.148 | <0.001 | <0.001 | 0.244 | 0.035 | 0.012 | 0.104 | 0.434 | 0.811 | 0.035 |
| miR-146a-5p | r | 0.098 | 1.000 | -0.173 | -0.221 | 0.330 | -0.211 | 0.065 | 0.590 | 0.054 | 0.440 | 0.405 |
| | p | 0.148 | NA | 0.010 | 0.001 | <0.001 | 0.002 | 0.342 | <0.001 | 0.429 | <0.001 | <0.001 |
| miR-155 | r | 0.222 | -0.173 | 1.000 | 0.832 | -0.437 | 0.792 | 0.153 | -0.314 | 0.055 | -0.439 | -0.331 |
| | p | <0.001 | 0.010 | NA | <0.001 | <0.001 | <0.001 | 0.023 | <0.001 | 0.417 | <0.001 | <0.001 |
| miR-195-5p | r | 0.313 | -0.221 | 0.832 | 1.000 | -0.488 | 0.752 | 0.253 | -0.393 | 0.056 | -0.539 | -0.394 |
| | p | <0.001 | 0.001 | <0.001 | NA | <0.001 | <0.001 | <0.001 | <0.001 | 0.409 | <0.001 | <0.001 |
| miR-21-5p | r | 0.079 | 0.330 | -0.437 | -0.488 | 1.000 | -0.419 | -0.007 | 0.686 | 0.055 | 0.723 | 0.686 |
| | p | 0.244 | <0.001 | <0.001 | <0.001 | NA | <0.001 | 0.913 | <0.001 | 0.417 | <0.001 | <0.001 |
| miR-24-3p | r | 0.143 | -0.211 | 0.792 | 0.752 | -0.419 | 1.000 | 0.232 | -0.353 | 0.034 | -0.479 | -0.355 |
| | p | 0.035 | 0.002 | <0.001 | <0.001 | <0.001 | NA | <0.001 | <0.001 | 0.615 | <0.001 | <0.001 |
| miR-320a | r | 0.169 | 0.065 | 0.153 | 0.253 | -0.007 | 0.232 | 1.000 | 0.027 | -0.056 | -0.140 | 0.136 |
| | p | 0.012 | 0.342 | 0.023 | <0.001 | 0.913 | <0.001 | NA | 0.696 | 0.409 | 0.039 | 0.044 |
| miR-342-3p | r | 0.110 | 0.590 | -0.314 | -0.393 | 0.686 | -0.353 | 0.027 | 1.000 | 0.015 | 0.741 | 0.720 |
| | p | 0.104 | <0.001 | <0.001 | <0.001 | <0.001 | <0.001 | 0.696 | NA | 0.825 | <0.001 | <0.001 |
| miR-376a | r | -0.053 | 0.054 | 0.055 | 0.056 | 0.055 | 0.034 | -0.056 | 0.015 | 1.000 | 0.068 | 0.073 |
| | p | 0.434 | 0.429 | 0.417 | 0.409 | 0.417 | 0.615 | 0.409 | 0.825 | NA | 0.320 | 0.282 |
| miR-422a | r | -0.016 | 0.440 | -0.439 | -0.539 | 0.723 | -0.479 | -0.140 | 0.741 | 0.068 | 1.000 | 0.632 |
| | p | 0.811 | <0.001 | <0.001 | <0.001 | <0.001 | <0.001 | 0.039 | <0.001 | 0.320 | NA | <0.001 |
| miR-451a | r | 0.143 | 0.405 | -0.331 | -0.394 | 0.686 | -0.355 | 0.136 | 0.720 | 0.073 | 0.632 | 1.000 |
| | p | 0.035 | <0.001 | <0.001 | <0.001 | <0.001 | <0.001 | 0.044 | <0.001 | 0.282 | <0.001 | NA |